
SCALABLE FEATURE LEARNING ON HUGE KNOWLEDGE GRAPHS FOR DOWNSTREAM MACHINE LEARNING

Félix Lefebvre
SODA Team, Inria Saclay
felix.lefebvre@inria.fr

Gaël Varoquaux
SODA Team, Inria Saclay
Probabl.ai
gael.varoquaux@inria.fr

ABSTRACT

Many machine learning tasks can benefit from external knowledge. Large knowledge graphs store such knowledge, and embedding methods can be used to distill it into ready-to-use vector representations for downstream applications. For this purpose, current models have however two limitations: they are primarily optimized for link prediction, via local contrastive learning, and they struggle to scale to the largest graphs due to GPU memory limits. To address these, we introduce SEPAL: a Scalable Embedding Propagation ALgorithm for large knowledge graphs designed to produce high-quality embeddings for downstream tasks at scale. The key idea of SEPAL is to enforce global embedding alignment by optimizing embeddings only on a small core of entities, and then propagating them to the rest of the graph via message passing. We evaluate SEPAL on 7 large-scale knowledge graphs and 46 downstream machine learning tasks. Our results show that SEPAL significantly outperforms previous methods on downstream tasks. In addition, SEPAL scales up its base embedding model, enabling fitting huge knowledge graphs on commodity hardware.

1 Introduction: embedding knowledge for downstream tasks

Bringing general knowledge to a machine-learning task revives an old promise of making it easier via this knowledge (Lenat and Feigenbaum, 2000). Data science is often about entities of the world – persons, places, organizations– that are increasingly well characterized in general-purpose knowledge graphs. These graphs carry rich information, including numerical attributes and relationships between entities, and can be connected to string values in tabular data through entity linking techniques (Mendes et al., 2011; Foppiano and Romary, 2020; Delpuch, 2019). However, integrating the corresponding data into tabular machine learning often raises the thorny challenge of assembling features from a relational graph (Kanter and Veeramachaneni, 2015; Cappuzzo et al., 2025; Robinson et al., 2025). Graph embedding methods offer a solution by distilling the graph information into node features readily usable by any downstream tabular learner (Grover and Leskovec, 2016; Cvetkov-Iliev et al., 2023; Ruiz et al., 2024).

The rapid growth of general-purpose knowledge graphs brings the exciting prospect of a very *general* feature enrichment. Indeed, the richer the knowledge graph, the more it can provide value to the downstream analysis (Ruiz et al., 2024). ConceptNet pioneered the distribution of general-knowledge embeddings, building on a graph of 8 million entities (Speer et al., 2017). As of 2025, Wikidata (Vrandečić and Krötzsch, 2014) describes 115M entities, and YAGO4 gives a curated view on 67M entities (Pelissier Tanon et al., 2020). Moreover, these knowledge graphs are rapidly expanding, with Wikidata alone gaining around 15M entities yearly (Wikimedia).

In parallel, the sophistication of knowledge-graph embedding (KGE) models is increasing (Bordes et al., 2013; Yang et al., 2015; Balazevic et al., 2019b, ...), capturing better the relational aspect of the data,

important for downstream tasks (Cvetkov-Iliev et al., 2023). However, much of the KGE literature remains focused on link prediction, a task shown to correlate poorly with the utility of the embeddings on real-world downstream tasks (Ruffinelli and Gemulla, 2024). One reason may be that, for link prediction, models typically optimize for local contrasts, resulting in embeddings that are not calibrated (Tabacof and Costabello, 2020).

Another challenge is that embedding models do not scale easily. There can be a disconnect between the growth of knowledge graphs, and the fact that increasingly complex embedding models tend to be less tractable, and are typically demonstrated on comparatively small graphs, subsets of real-world graphs such as FB15k (15k entities from Freebase) or WN18 (40k entities from WordNet), three orders of magnitude smaller than modern general knowledge graphs or industrial knowledge graphs (Sullivan, 2020). The typical answer to this challenge is distributed computation across GPUs or machines, explored by PyTorch-BigGraph (Lerer et al., 2019) and many more (Zheng et al., 2020; Mohoney et al., 2021; Zhu et al., 2019; Dong et al., 2022; Ren et al., 2022; Zheng et al., 2024, ...). This comes with sizeable computational costs, as the graph is fit piece by piece, increasing the data movement across devices for entities involved in several edge partitions. Moreover, the hardware requirement is a challenge for non-profits such as the Wikimedia Foundation, in charge of Wikidata, given that the embeddings should be recomputed regularly to incorporate newly added entities.

Here we present a KGE approach to 1) capture better some global structure of the graph, 2) scale to huge graphs with little computational resources. This approach applies as a wrapper to many KGE methods. It bridges the gap between advances in embedding approaches and the goal to create large and reusable general-knowledge embeddings for downstream applications. For this, we leverage a fundamental structure in knowledge graphs: a small set of *core* entities comes with much more information than the others. Our method, SEPAL (Scalable Embedding Propagation ALgorithm), scales up any embedding model that, at triple-level, models the tail embedding as a relation-specific transformation of the head embedding. Two technical contributions are key to SEPAL’s scalability. 1) Time-wise: we show that message passing, rather than classic optimization, can be used to propagate embeddings of a small core subset of entities and give good embeddings for the full graph. The challenge here is to maintain the relational geometry. 2) Memory-wise: we devise an algorithm called BLOCS to break down a huge knowledge graph into overlapping subsets that fit in GPU memory. Here, the challenge lies in the scale-free and connectivity properties of a large knowledge graph: some nodes are connected to a significant fraction of the graph, while others are very hard to reach.

We start by reviewing related work. Then, section 3 describes our contributed method and section 4 gives a theoretical analysis. In section 5 we evaluate SEPAL’s performance on knowledge graphs of increasing size between YAGO3 (2.6M entities, Mahdisoltani et al., 2014) and WikiKG90Mv2 (91M entities, Hu et al., 2020); we study the use of the embeddings for feature enrichment on 46 downstream machine learning tasks, showing that SEPAL makes embedding methods more tractable while generating better embeddings for downstream tasks. Finally, section 6 discusses the contributions and limitations of SEPAL. Empirical findings show that:

1. SEPAL’s propagation of core embeddings to outer entities with message passing improves the downstream performance compared to classic optimization;
2. this approach can be scaled to very large knowledge graphs on modest hardware. We embed WikiKG90Mv2 –91M entities, 601M triples– with a single 32GB V100 GPU.

2 Related work: embedding and scalability

Knowledge graphs are multi-relational graphs storing information as triples (h, r, t) , where h is the head entity, r is the relation, and t is the tail entity. We denote \mathcal{V} and \mathcal{R} respectively the set of entities and relations, and \mathcal{K} the set of triples of a given knowledge graph ($\mathcal{K} \subset \mathcal{V} \times \mathcal{R} \times \mathcal{V}$).

2.1 Embedding knowledge graphs

Here, we provide an overview of approaches to generate low-dimensional (typically $d = 100$ or 200) vector representations for the entities, that can be used in downstream applications. These include both graph-embedding techniques, that leave aside the relations, and knowledge-graph embedding (KGE) methods accounting for relations.

Table 1: Expression of ϕ in some embedding models. \odot denotes the Hadamard product, \otimes the Hamilton product, and \times_i the tensor product along mode i . The models we list here are all compatible with our proposed SEPAL approach.

Model	Relational operator ϕ
TransE (Bordes et al., 2013)	$\theta_h + w_r$
MuRE (Balazevic et al., 2019b)	$\theta_h \odot \rho_r - w_r$
RotatE (Sun et al., 2019)	$\theta_h \odot w_r$
QuatE (Zhang et al., 2019)	$\theta_h \otimes w_r$
DistMult (Yang et al., 2015)	$\theta_h \odot w_r$
ComplEx (Trouillon et al., 2016)	$\theta_h \odot w_r$
TuckER (Balazevic et al., 2019a)	$\mathcal{W} \times_1 \theta_h \times_2 w_r$

Graph embedding A first simple strategy to get very cost-effective vector representations is to compute **random projections**. This avoids relying on –potentially costly– optimization, and provides embeddings preserving the pairwise distances to within an epsilon (Dasgupta and Gupta, 2003). FastRP (Chen et al., 2019a) proposes a scalable approach, with a few well-chosen very sparse random projections of the normalized adjacency matrix and its powers.

Another family of methods performs explicit **matrix factorizations** on matrices derived from the adjacency matrix, for instance GraREP (Cao et al., 2015) or NetMF (Qiu et al., 2018). These methods output close embedding vectors for nodes with similar neighborhoods.

Similarly, **Skip-Gram Negative Sampling** (SGNS), behind word2vec (Mikolov et al., 2013a,b), performs an implicit factorization (Levy and Goldberg, 2014). It has been adapted to graphs: DeepWalk (Perozzi et al., 2014) and node2vec (Grover and Leskovec, 2016) use random walks on the graph to generate “sentences” fed to word2vec. LINE (Tang et al., 2015) explores a similar strategy varying edge sampling.

Knowledge-graph embedding RDF2vec (Ristoski and Paulheim, 2016) adapts SGNS to multi-relational graphs by simply adding the relations to the generated sentences.

More advanced methods model relations as geometric transformations in the embedding space. These **triple-based methods**, inspired by SGNS, represent the plausibility of a triple given the embeddings θ_h, w_r, θ_t of the entities and relation with a scoring function $f(h, r, t)$ often written as

$$\text{Scoring function} \quad f(h, r, t) = -\text{sim}(\phi(\theta_h, w_r), \theta_t) \tag{1}$$

where ϕ is a model-specific relational operator, and sim a similarity function. The embeddings are optimized by gradient descent to maximize the score of positive triples, and minimize that of negative ones. These models strive to align, for positive triples, the tail embedding θ_t with the “relationally” transformed head embedding $\phi(\theta_h, w_r)$. The challenge is to design a clever ϕ operator to model complex patterns in the data –hierarchies, compositions, symmetries... Indeed some relations are one-to-one (people only have one biological mother), well represented by a translation (Bordes et al., 2013), while others are many-to-one (for instance many person were BornIn Paris), calling for ϕ to contract distances (Wang et al., 2017). Many models explore different parametrizations, among which MuRE (Balazevic et al., 2019b), RotatE (Sun et al., 2019), or QuatE (Zhang et al., 2019) have good performance (Ali et al., 2021a). This framework also includes models like DistMult (Yang et al., 2015), ComplEx (Trouillon et al., 2016), or TuckER (Balazevic et al., 2019a), that implicitly perform tensor factorizations.

Embedding propagation To smooth computed embeddings, CompGCN (Vashishth et al., 2020) introduces the idea of propagating knowledge-graph embeddings using the relational operator ϕ , but couples it with learnable weights and a non-linearity. REP (Wang et al., 2022) simplifies this framework by removing weight matrices and non-linearities. Rossi et al. (2022) also uses Feature Propagation, but to impute missing node features in graphs.

2.2 Techniques for scaling graph algorithms

Various tricks help scale graph algorithms to the sizes we are interested in –millions of nodes.

Graph partitioning Scaling up graph computations, for graph embedding or more generally, often relies on breaking down graphs in subgraphs. Appendix E.1 presents corresponding prior work.

Local subsampling Other forms of data reduction can help to scale graph algorithms (*e.g.* based on message passing). Algorithms may subsample neighborhoods, as GraphSAGE (Hamilton et al., 2017) that selects a fixed number of neighbors for each node on each layer, or MariusGNN (Wal-effe et al., 2023) that uses an optimized data structure for neighbor sampling and GNN aggregation. Cluster-GCN (Chiang et al., 2019) restricts the neighborhood search within clusters, obtained by classic clustering algorithms, to improve computational efficiency. GraphSAINT (Zeng et al., 2020) samples overlapping subgraphs through random walks, for supervised GNN training via node classification, optimizing GNN weights without processing the full graph.

Multi-level techniques Multi-level approaches, such as HARP (Chen et al., 2018), GraphZoom (Deng et al., 2020) or MILE (Liang et al., 2021), coarsen the graph, compute embeddings on the smaller graph, and project them back to the original graph.

2.3 Scaling knowledge-graph embedding

Parallel training Many approaches scale triple-level stochastic solvers by distributing training across multiple workers, starting from the seminal PyTorch-BigGraph (PBG) (Lerer et al., 2019) that splits the triples into buckets based on the partitioning of the entities. The challenge is then to limit overheads and communication costs coming from 1) the additional data movement incurred by embeddings of entities occurring in several buckets 2) the synchronization of global trainable parameters such as the relation embeddings. For this, DGL-KE (Zheng et al., 2020) reduces data movement by using sparse relation embeddings and METIS graph partitioning (Karypis and Kumar, 1997) to distribute the triples across workers. HET-KG (Dong et al., 2022) further optimizes distributed training by preserving a copy of the most frequently used embeddings on each worker, to reduce communication costs. These “hot-embeddings” are periodically synchronized to minimize inconsistency. SMORE (Ren et al., 2022) leverages asynchronous scheduling to overlap CPU-based data sampling, with GPU-based embedding computations. Algorithmically, it contributes a rejection sampling strategy to generate the negatives at low cost. GraphVite (Zhu et al., 2019) accelerates SGNS for graph embedding by both parallelizing random walk sampling on multiple CPUs, and negative sampling on multiple GPUs. Marius (Mohoney et al., 2021) reduces synchronization overheads by opting for asynchronous training of entity embeddings with bounded staleness, and minimizes IO with partition caching and buffer-aware data ordering. GE2 (Zheng et al., 2024) improves data swap between CPU and multiple GPUs. Finally, the LibKGE (Broscheit et al., 2020) Python library also supports parallel training and includes GraSH (Kochsiek et al., 2022), an efficient hyperparameter optimization algorithm for large-scale KGE models.

Parameter-efficient methods Other approaches reduce GPU memory pressure by limiting the number of parameters. NodePiece (Galkin et al., 2022) and EARL (Chen et al., 2023) embed a subset of entities and train an encoder to compute the embeddings of the other entities. However, their tokenization step is costly, and they have not been demonstrated on graphs larger than 2.5M nodes.

3 SEPAL: expanding from a core subgraph

Most work on scaling knowledge-graph embedding has focused on efficient parallel computing to speed up stochastic optimization. We introduce a different approach, SEPAL, which changes how embeddings are computed, enforcing a more global structure, beneficial for downstream tasks, while avoiding much of the optimization cost. To that end, SEPAL proceeds in three steps (Figure 1):

1. separates the graph in a core and a set of connected overlapping outer subgraphs that cover the full graph;
2. uses a classic KGE model to optimize the embeddings of the core entities and relations;
3. propagates the embeddings from the core to the outer subgraphs, using a message-passing strategy preserving the relational geometry and ensuring global embedding consistency, with no further training.

SEPAL’s key idea is to allocate more computation time to the more frequent entities and then use message passing to propagate embeddings at low cost to regions of the graph where they have not been computed yet. It departs from existing embedding propagation methods (Vashishth et al., 2020; Wang et al., 2022) that compute embeddings on the full graph and use propagation as post-processing

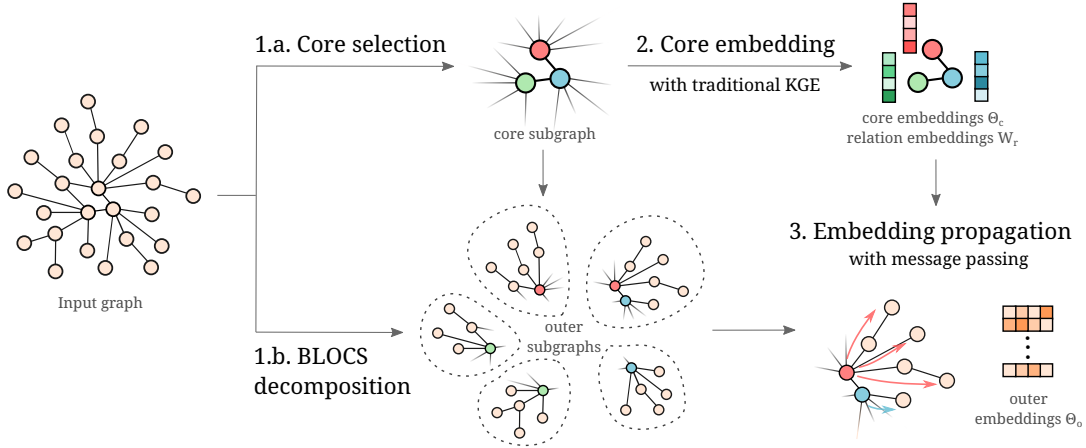


Figure 1: **SEPAL’s embedding pipeline.** First, a core subgraph is extracted from the input knowledge graph (step 1.a). BLOCS then subdivides this input knowledge graph into outer subgraphs (step 1.b). Next, the core subgraph is embedded using traditional KGE models, which generate vector representations for both core entities and relations (step 2.). Finally, these embeddings are propagated with message passing to each outer subgraph successively (step 3.).

to smooth them. SEPAL is compatible with any embedding model whose scoring function has the form given by Equation 1, examples of which are provided in Table 1.

3.1 Splitting large graphs into manageable subgraphs

Breaking up the graph into subgraphs is key to scaling up our approach memory-wise. Specifically, we seek a set of subgraphs that altogether cover the full graph but are individually small enough to fit on GPUs, to enable the subsequent GPU-based message passing.

Core subgraph SEPAL first defines the *core* of a knowledge graph. The quality of the core embeddings is particularly important, as they serve as (fixed) boundary conditions during the propagation phase. To optimize this quality, two key factors must be considered during core selection: 1) ensuring a dense core subgraph by selecting the most central entities and 2) achieving full coverage of relation types. Yet, there can be a trade-off between these two objectives, hence, SEPAL offers two core selection procedures:

Degree-based selection: This simple approach selects the top entities by degree –with proportion $\eta_n \in (0, 1)$ – and keeps only the largest connected component of the induced subgraph. The resulting core is dense, which boosts performance for entity-centric tasks like feature enrichment (Appendix F.2). However, it does not necessarily contain all the relation types.

Hybrid selection: To ensure full relational coverage, this method combines two sampling strategies. First, it selects entities with the highest η_n degrees. Second, for each relation type, it includes entities involved in edges with the highest η_e degrees (where degree is the sum of the head and tail nodes’ degrees). The union of these two sets forms the core, and if disconnected, SEPAL reconnects it by adding the necessary entities (details in Appendix F.2). Hyperparameters $\eta_n, \eta_e \in (0, 1)$ are proportions of nodes and edges that control the core size.

Compared to degree-based selection, hybrid selection benefits tasks relying on relation embeddings, such as link prediction. However, its additional relation-specific edge sampling and reconnection steps can be computationally expensive for knowledge graphs with many relations.

Outer subgraphs The next class of subgraphs that we generate –the *outer* subgraphs– aim at covering the rest of the graph. The purpose of these subgraphs demands the following requirements:

R1: connected the subgraphs must be connected, to propagate the embeddings;

R2: bounded size the subgraphs must have bounded sizes, to fit their embeddings in GPU memory;

R3: coverage the union of the subgraphs must be the full graph, to embed every entity;

R4: scalability extraction must run with available computing resources, in particular memory.

Extracting such subgraphs is challenging on large knowledge graphs. These are scale-free graphs with millions of nodes and no well-defined clusters (Leskovec et al., 2009). They pose difficulties to partitioning algorithms. For instance, algorithms based on propagation, eigenvalues, or power iterations of the adjacency matrix (Raghavan et al., 2007; Shi and Malik, 2000; Newman, 2006) struggle with the presence of extremely high-degree nodes that make the adjacency matrix ill-conditioned. None of the existing partitioning algorithms satisfy our full set of constraints, and thus we devise our own algorithm, called BLOCS and described in detail in Appendix E. To satisfy the requirements despite these challenges, BLOCS creates *overlapping* subgraphs.

3.2 Core optimization with traditional KGE models

Once the core subgraph is defined, SEPAL trains on GPU any compatible triple-based embedding model (DistMult, TransE, ...). This process generates embeddings for the core entities and relations, including inverse relations, added to ensure connectedness for the subsequent propagation step.

3.3 Outside the core: relation-aware propagation

Key to SEPAL’s global consistency of embeddings and to computational efficiency is that it does not use contrastive learning and gradient descent for the outer entities. Instead, the final step involves an embedding propagation that is consistent with the KGE model (multiplication for DistMult, addition for TransE, ...) and preserves the relational geometry of the embedding space. To do so, SEPAL leverages the entity-relation composition function ϕ (given by Table 1) used by the KGE model, and the embeddings of the relations w_r trained on the core subgraph. From Equation 1 one can derive, for a given triple (h, r, t) , the closed-form expression of the tail embedding that maximizes the scoring function $\arg \max_{\theta_t} f(h, r, t) = \phi(\theta_h, w_r)$. SEPAL uses this property to compute outer embeddings as consistent with the core as possible, by propagating from core entities with message passing.

First, the embeddings are initialized with
$$\theta_u^{(0)} = \begin{cases} \theta_u, & \text{if entity } u \text{ belongs the core subgraph,} \\ \mathbf{0}, & \text{otherwise.} \end{cases}$$

Then, each outer subgraph $\mathcal{S} \subset \mathcal{K}$ is loaded on GPU, merged with the core subgraph \mathcal{C} , and SEPAL performs T steps of propagation (T is a hyperparameter), with the following message-passing equations:

$$\text{Message:} \quad m_{v,u}^{(t+1)} = \sum_{(v,r,u) \in \mathcal{S} \cup \mathcal{C}} \phi(\theta_v^{(t)}, w_r) \quad (2)$$

$$\text{Aggregation:} \quad a_u^{(t+1)} = \sum_{v \in \mathcal{N}(u)} m_{v,u}^{(t+1)} \quad (3)$$

$$\text{Update:} \quad \theta_u^{(t+1)} = \frac{\theta_u^{(t)} + \alpha a_u^{(t+1)}}{\left\| \theta_u^{(t)} + \alpha a_u^{(t+1)} \right\|_2} \quad (4)$$

where $\mathcal{N}(u)$ denotes the set of neighbors of outer entity u , \mathcal{K} the set of positive triples of the graph, and α a hyperparameter similar to a learning rate. During updates, ℓ_2 normalization projects embeddings on the unit sphere. With DistMult, this accelerates convergence by canceling the effect of neighbors that still have zero embeddings. Normalizing embeddings is a common practice in knowledge-graph embedding (Bordes et al., 2013; Yang et al., 2015), and SEPAL acts accordingly. During propagation, the core embeddings remain frozen.

4 Theoretical analysis

SEPAL minimizes a global energy via gradient descent Proposition 4.1 shows that SEPAL with DistMult minimizes an energy that only accounts for the positive triples. The more aligned the embeddings within positive triples, the lower this energy. In self-supervised learning, negative sampling is needed to prevent embeddings from collapsing to a single point (Hafidi et al., 2022). However, in our case, this oversmoothing is avoided thanks to the boundary conditions of fixed core-entities and relations embeddings, which act as “anchors” in the embedding space.

Proposition 4.1 (Implicit Gradient Descent). *Let \mathcal{E} be the “alignment energy” defined as*

$$\mathcal{E} = - \sum_{(h,r,t) \in \mathcal{K}} \langle \theta_t, \phi(\theta_h, \mathbf{w}_r) \rangle, \quad (5)$$

with $\phi(\theta_h, \mathbf{w}_r) = \theta_h \odot \mathbf{w}_r$ being the *DistMult* relational operator. Then, *SEPAL’s propagation step amounts to a mini-batch projected gradient step descending \mathcal{E} under the following conditions:*

1. *SEPAL uses DistMult as base KGE model;*
2. *the embeddings of relations and core entities remain fixed, and serve as boundary conditions;*
3. *the outer subgraphs act as mini-batches.*

Proof sketch. For an outer entity u , the gradient update of its embedding $\theta_u^{(t+1)} = \theta_u^{(t)} - \eta \frac{\partial \mathcal{E}}{\partial \theta_u^{(t)}}$ boils down to *SEPAL’s* propagation equation, for a learning rate $\eta = \alpha$. See Appendix D.2 for detailed derivations. \square

Analogy to eigenvalue problems Appendix D.1 shows that *SEPAL’s* propagation, when combined with *DistMult*, resembles an Arnoldi-like iteration, suggesting that entity embeddings converge toward generalized eigenvectors of an operator that integrates both global graph structure and relation semantics (via fixed relation embeddings).

Queriability of embeddings Assume that each entity $u \in \mathcal{V}$ is associated with a set of scalar features $\mathbf{x}_u \in \mathbb{R}^m$, such that $x_{u,i}$ denotes the i -th property of u . We say that the embeddings support *queriability* with respect to property $i \in 1, \dots, m$ if,

$$\exists f_i \in \mathcal{F} \quad \text{such that} \quad f_i(\theta_u) \approx x_{u,i}, \quad (6)$$

where \mathcal{F} denotes a class of functions from \mathbb{R}^d to \mathbb{R} constrained by some regularity conditions. This queriability property is key to the embeddings’ utility to downstream machine learning tasks.

In knowledge graphs, properties $x_{u,i}$ that are explicitly represented by triples (u, r_i, v_i) can be recovered via the scoring function ϕ used in the model, under the condition of well-aligned embeddings. Specifically, when such a relation r_i exists, a natural querying function is

$$f_i : \mathbf{x} \mapsto \phi(\mathbf{x}, \mathbf{w}_{r_i}) \quad (7)$$

where \mathbf{w}_{r_i} is the embedding of relation r_i (we assume scalar embeddings for simplicity).

Proposition 4.1 shows that *SEPAL* minimizes an energy that promotes global alignment between embeddings of positive triples, leading to embeddings with high queriability. In contrast, classic KGE methods use negative sampling to incorporate a supplementary constraint of local contrast between positive and negative triples. This adds discriminative power to the model, useful for link prediction, but can be detrimental to the global alignment of embeddings, which is important for queriability.

5 Experimental study: utility to downstream task and scalability

Knowledge graph datasets To compare large knowledge graphs of different sizes, we use Freebase (Bollacker et al., 2008), WikiKG90Mv2 ((an extract of Wikidata) Hu et al., 2020), and three generations of YAGO: YAGO3 (Mahdisoltani et al., 2014), YAGO4 (Pellissier Tanon et al., 2020), and YAGO4.5 (Suchanek et al., 2024). We expand YAGO4 and YAGO4.5 into a larger version containing also the taxonomy, i.e., types and classes –which algorithms will treat as entities– and their relations. We discard numerical attributes and keep only the largest connected component (Appendix A.1). To perform an ablation study of *SEPAL* without BLOCS for which we need smaller datasets, we also introduce Mini YAGO3, a subset of YAGO3 built with the 5% most frequent entities. Knowledge graph sizes are reported in Figure 5.

On real-world downstream regression tasks We evaluate the embeddings as node features in downstream tasks (Grover and Leskovec, 2016; Cvetkov-Iliev et al., 2023; Robinson et al., 2025; Ruiz et al., 2024). Specifically, we incorporate the embeddings in tables as extra features and measure the prediction improvement of a standard estimator in regression tasks. This setup allows us to compare the utility

of knowledge graphs of varying sizes. Indeed, for a task, a suboptimal embedding of a larger knowledge graph may be more interesting than a high-quality embedding of a smaller knowledge graph because the larger graph brings richer information, on more entities. We benchmark 4 downstream regression tasks (adapted from Cvetkov-Iliev et al., 2023): Movie revenues, US accidents, US elections, and housing prices. Details are provided in Appendix A.2.

Larger knowledge graphs do bring value (Figure 2), as they cover more entities of the downstream tasks (Figure 4). For each source graph, SEPAL provides the best embeddings and is much more scalable (details in Figure 5). Considering performance/cost Pareto optimality across methods and source graphs (Figure 2a), SEPAL achieves the best performance with reduced cost, but the simple baseline FastRP also gives Pareto-optimal results, for smaller costs. Although FastRP discards the type of relation, it performs better than most dedicated KGE methods. Its iterations also solve a more global problem, like SEPAL (Appendix D.1).

We used DistMult as base model as it is a classic and good performer (Ruffinelli et al., 2020; Kadlec et al., 2017; Jain et al., 2020). Figure 22 shows that SEPAL can speed up DistMult over 20 times for a given training configuration. For other scoring functions like RotatE and TransE, Figure 7 shows that SEPAL also improves the downstream performance of its base model.

On WikiDBs tables We also evaluate SEPAL on tables from WikiDBs (Vogel et al., 2024), a corpus of databases extracted from Wikidata. We build 42 downstream tables (26 classification tasks, and 16 regression tasks), described in Appendix A.2. Four of them are used as validation tasks, to tune hyperparameters, and the remaining 38 are used as test tables. Figure 3 presents the aggregated results on these 38 test tables, showing that, here also, applying SEPAL to very large graphs provides the best embeddings for downstream node regression and classification, and that SEPAL brings a decreased computational cost. Regarding the performance-cost tradeoff, FastRP is once again Pareto-optimal for small computation times, highlighting the benefits of global methods.

6 Discussion and conclusion

Benefits of larger graphs We have studied how to build general-knowledge feature enrichment from huge knowledge graphs. For this purpose, we have introduced a scalable method that captures more of the global structure than the classic KGE methods. Our results show the benefit of embedding larger graphs. There are two reasons to this benefit: (1) larger knowledge graphs can result in larger coverage of downstream entities (another important factor for this is the age of the dataset: recent ones have better coverage) (2) for two knowledge graphs with equal coverage, the larger one can result in richer representations because the covered entities have more context to learn from.

Limitations Our work focuses on embeddings for feature enrichment of downstream tables, an active research field (Cvetkov-Iliev et al., 2023; Ruiz et al., 2024; Robinson et al., 2025). Another popular use case for embeddings is knowledge graph completion. However, this task is fundamentally different

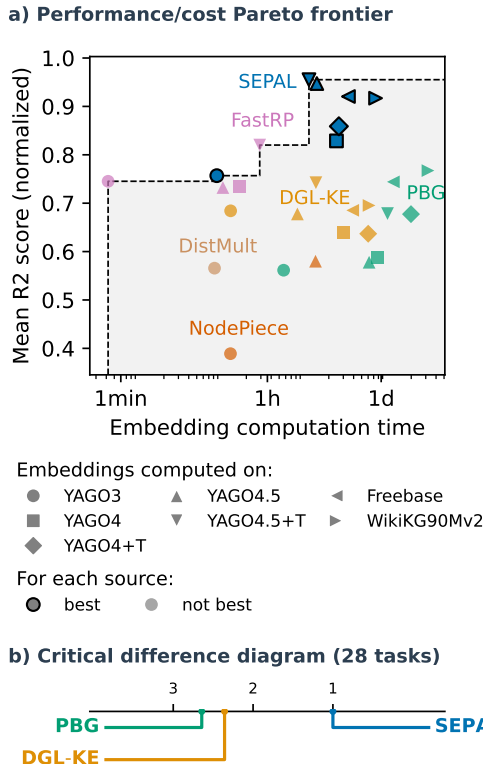


Figure 2: **Statistical performance on real-world tables.** **a) Pareto frontiers** of averaged normalized prediction scores with respect to embedding times (log-scale). **b) Critical difference diagrams** (Terpilowski, 2019) of average ranks among the three methods (SEPAL, PBG and DGL-KE) that scale to every knowledge-graph dataset. The ranks are averaged over all tasks; a task being defined as the combination of a downstream table and a source knowledge graph. SEPAL gets the best average downstream performance for each of the 7 source knowledge graphs. Figure 5 gives the detailed results for each table. Appendix B.1 details the metric used.

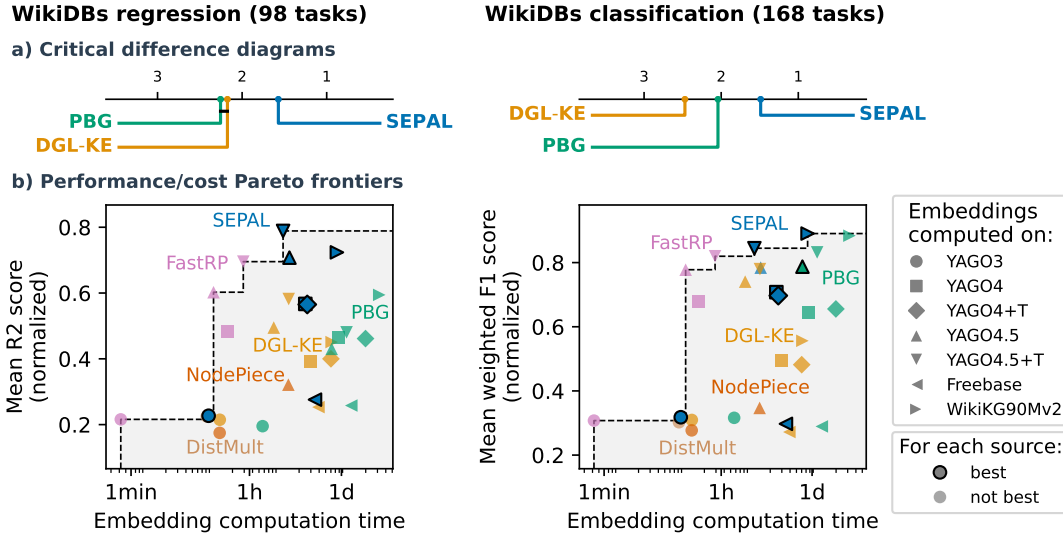


Figure 3: **Statistical performance on WikiDBs tables.** **a) Critical difference diagrams** of scalable methods. Black lines connect methods that are not significantly different. **b) Pareto frontiers** of averaged normalized prediction scores with respect to embedding times (log-scale). Figure 6 in Appendix C.2 provides the detailed results for each of the 38 test tables.

from feature enrichment: embeddings optimized for link prediction may not perform well for feature enrichment, and vice versa (Ruffinelli and Gemulla, 2024). Nevertheless, we also evaluate SEPAL on knowledge graph completion, for which we expect lower performances given that SEPAL does not locally optimize the contrast between positive and negative triples scores. Results reported in Appendix C.4 show that SEPAL sometimes performs lower than existing methods (DGL-KE, PBG) on this task, although no method is consistently better than the others for all datasets, and statistical tests show no significant differences (Figure 8).

Conclusion: for downstream machine learning, embeddings should be optimized globally In this paper, we show how to optimize knowledge-graph embeddings for downstream machine learning. We propose a very scalable method, SEPAL, and conduct a comprehensive evaluation on 7 knowledge graphs and 46 downstream tables showing that SEPAL both: (1) markedly improves predictive performance on downstream tasks and (2) brings computational-performance benefits—multiple-fold decreased train times and bounded memory usage—when embedding large-scale knowledge graphs. Our theoretical analysis suggests that SEPAL’s strong performance on downstream tasks stems from its global optimization approach, resulting in better-aligned embeddings compared to classic methods based on negative sampling. SEPAL improves the quality of the generated node features when used for data enrichment in external (downstream) tasks, a setting that can strongly benefit from pre-training embeddings on knowledge bases as large as possible. It achieves this without requiring heavy engineering, such as distributed computing, and can easily be adapted to most KGE models.

Insights brought by our experiments go further than SEPAL. First, the method successfully exploits the asymmetry of information between “central” entities and more peripheral ones. Power-law distributions are indeed present on many types of objects, from words (Piantadosi, 2014) to geographical entities (Giesen and Südekum, 2011) and should probably be exploited for general-knowledge representations such as knowledge-graph embeddings. Second, and related, breaking up large knowledge graphs in communities is surprisingly difficult: some entities just belong in many (all?) communities, and others are really hard to reach. Our BLOCS algorithm can be useful for other graph engineering tasks, such as scaling message-passing algorithms or simply generating partitions. Finally, the embedding propagation in SEPAL appears powerful, and we conjecture it will benefit further approaches. First, it can be combined with much of the prior art to scale knowledge-based embedding. Second, it could naturally adapt to continual learning settings (Van de Ven et al., 2022; Hadsell et al., 2020; Biswas et al., 2023),

which are important in knowledge-graph applications since knowledge graphs, such as Wikidata, are often continuously updated with new information.

References

- M. Ali, M. Berrendorf, C. T. Hoyt, L. Vermue, M. Galkin, S. Sharifzadeh, A. Fischer, V. Tresp, and J. Lehmann. Bringing light into the dark: A large-scale evaluation of knowledge graph embedding models under a unified framework. *IEEE Transactions on Pattern Analysis and Machine Intelligence*, 44(12):8825–8845, 2021a.
- M. Ali, M. Berrendorf, C. T. Hoyt, L. Vermue, S. Sharifzadeh, V. Tresp, and J. Lehmann. PyKEEN 1.0: A Python Library for Training and Evaluating Knowledge Graph Embeddings. *Journal of Machine Learning Research*, 22(82):1–6, 2021b. URL <http://jmlr.org/papers/v22/20-825.html>.
- W. E. Arnoldi. The principle of minimized iterations in the solution of the matrix eigenvalue problem. *Quarterly of applied mathematics*, 9(1):17–29, 1951.
- I. Balazevic, C. Allen, and T. Hospedales. TuckER: Tensor factorization for knowledge graph completion. In K. Inui, J. Jiang, V. Ng, and X. Wan, editors, *Proceedings of the 2019 Conference on Empirical Methods in Natural Language Processing and the 9th International Joint Conference on Natural Language Processing (EMNLP-IJCNLP)*, pages 5185–5194, Hong Kong, China, Nov. 2019a. Association for Computational Linguistics. doi: 10.18653/v1/D19-1522. URL <https://aclanthology.org/D19-1522/>.
- I. Balazevic, C. Allen, and T. Hospedales. Multi-relational poincaré graph embeddings. *Advances in Neural Information Processing Systems*, 32, 2019b.
- D. P. Bertsekas. Nonlinear programming. *Journal of the Operational Research Society*, 48(3):334–334, 1997.
- R. Biswas, L.-A. Kaffee, M. Cochez, S. Dumbrava, T. E. Jendal, M. Lissandrini, V. Lopez, E. L. Mencía, H. Paulheim, H. Sack, et al. Knowledge graph embeddings: open challenges and opportunities. *Transactions on Graph Data and Knowledge*, 1(1):4–1, 2023.
- V. D. Blondel, J.-L. Guillaume, R. Lambiotte, and E. Lefebvre. Fast unfolding of communities in large networks. *Journal of statistical mechanics: theory and experiment*, 2008(10):P10008, 2008.
- K. Bollacker, C. Evans, P. Paritosh, T. Sturge, and J. Taylor. Freebase: a collaboratively created graph database for structuring human knowledge. In *Proceedings of the 2008 ACM SIGMOD international conference on Management of data*, pages 1247–1250, 2008.
- T. Bolukbasi, K.-W. Chang, J. Y. Zou, V. Saligrama, and A. T. Kalai. Man is to computer programmer as woman is to homemaker? debiasing word embeddings. *Advances in neural information processing systems*, 29, 2016.
- A. Bordes, N. Usunier, A. Garcia-Duran, J. Weston, and O. Yakhnenko. Translating embeddings for modeling multi-relational data. *Advances in neural information processing systems*, 26, 2013.
- S. Broscheit, D. Ruffinelli, A. Kochsiek, P. Betz, and R. Gemulla. LibKGE - A knowledge graph embedding library for reproducible research. In *Proceedings of the 2020 Conference on Empirical Methods in Natural Language Processing: System Demonstrations*, pages 165–174, 2020. URL <https://www.aclweb.org/anthology/2020.emnlp-demos.22>.
- S. Cao, W. Lu, and Q. Xu. Grarep: Learning graph representations with global structural information. In *Proceedings of the 24th ACM international on conference on information and knowledge management*, pages 891–900, 2015.
- R. Cappuzzo, A. Coelho, F. Lefebvre, P. Papotti, and G. Varoquaux. Retrieve, merge, predict: Augmenting tables with data lakes. *TMLR*, 2025.
- H. Chen, B. Perozzi, Y. Hu, and S. Skiena. Harp: Hierarchical representation learning for networks. In *Proceedings of the AAAI conference on artificial intelligence*, volume 32, 2018.
- H. Chen, S. F. Sultan, Y. Tian, M. Chen, and S. Skiena. Fast and accurate network embeddings via very sparse random projection. In *Proceedings of the 28th ACM international conference on information and knowledge management*, pages 399–408, 2019a.
- M. Chen, W. Zhang, Z. Yao, Y. Zhu, Y. Gao, J. Z. Pan, and H. Chen. Entity-agnostic representation learning for parameter-efficient knowledge graph embedding. In *Proceedings of the AAAI Conference on Artificial Intelligence*, volume 37, pages 4182–4190, 2023.

- R. Chen, J. Shi, Y. Chen, B. Zang, H. Guan, and H. Chen. Powerlyra: Differentiated graph computation and partitioning on skewed graphs. *ACM Transactions on Parallel Computing (TOPC)*, 5(3):1–39, 2019b.
- W.-L. Chiang, X. Liu, S. Si, Y. Li, S. Bengio, and C.-J. Hsieh. Cluster-gcn: An efficient algorithm for training deep and large graph convolutional networks. In *Proceedings of the 25th ACM SIGKDD international conference on knowledge discovery & data mining*, pages 257–266, 2019.
- W. J. Conover. *Practical nonparametric statistics*. john wiley & sons, 1999.
- W. J. Conover and R. L. Iman. Multiple-comparisons procedures. informal report. Technical report, Los Alamos National Lab.(LANL), Los Alamos, NM (United States), 1979.
- M. G. Csardi. Package ‘igraph’. *Last accessed*, 3(09):2013, 2013.
- A. Cvetkov-Iliev, A. Allauzen, and G. Varoquaux. Relational data embeddings for feature enrichment with background information. *Machine Learning*, 112(2):687–720, 2023.
- S. Dasgupta and A. Gupta. An elementary proof of a theorem of johnson and lindenstrauss. *Random Structures & Algorithms*, 22(1):60–65, 2003.
- A. Delpuech. Opentapioca: Lightweight entity linking for wikidata. *arXiv preprint arXiv:1904.09131*, 2019.
- C. Deng, Z. Zhao, Y. Wang, Z. Zhang, and Z. Feng. Graphzoom: A multi-level spectral approach for accurate and scalable graph embedding. In *International Conference on Learning Representations*, 2020. URL <https://openreview.net/forum?id=r1lG00EKDH>.
- S. Dong, X. Miao, P. Liu, X. Wang, B. Cui, and J. Li. Het-kg: Communication-efficient knowledge graph embedding training via hotness-aware cache. In *2022 IEEE 38th International Conference on Data Engineering (ICDE)*, pages 1754–1766. IEEE, 2022.
- J. Fisher, A. Mittal, D. Palfrey, and C. Christodoulopoulos. Debiasing knowledge graph embeddings. In *Proceedings of the 2020 Conference on Empirical Methods in Natural Language Processing (EMNLP)*, pages 7332–7345, 2020.
- L. Foppiano and L. Romary. entity-fishing: a dariah entity recognition and disambiguation service. *Journal of the Japanese Association for Digital Humanities*, 5(1):22–60, 2020.
- M. Galkin, E. Denis, J. Wu, and W. L. Hamilton. Nodepiece: Compositional and parameter-efficient representations of large knowledge graphs. In *International Conference on Learning Representations*, 2022. URL <https://openreview.net/forum?id=xMJWUKJnFSw>.
- K. Giesen and J. Südekum. Zipf’s law for cities in the regions and the country. *Journal of economic geography*, 11(4):667–686, 2011.
- A. Grover and J. Leskovec. node2vec: Scalable feature learning for networks. In *Proceedings of the 22nd ACM SIGKDD international conference on Knowledge discovery and data mining*, pages 855–864, 2016.
- R. Hadsell, D. Rao, A. A. Rusu, and R. Pascanu. Embracing change: Continual learning in deep neural networks. *Trends in cognitive sciences*, 24(12):1028–1040, 2020.
- H. Hafidi, M. Ghogho, P. Ciblat, and A. Swami. Negative sampling strategies for contrastive self-supervised learning of graph representations. *Signal Processing*, 190:108310, 2022.
- W. Hamilton, Z. Ying, and J. Leskovec. Inductive representation learning on large graphs. *Advances in neural information processing systems*, 30, 2017.
- W. Hu, M. Fey, M. Zitnik, Y. Dong, H. Ren, B. Liu, M. Catasta, and J. Leskovec. Open graph benchmark: Datasets for machine learning on graphs. *Advances in neural information processing systems*, 33:22118–22133, 2020.
- P. Jain, S. Rathi, S. Chakrabarti, et al. Knowledge base completion: Baseline strikes back (again). *arXiv preprint arXiv:2005.00804*, 2020.
- R. Kadlec, O. Bajgar, and J. Kleindienst. Knowledge base completion: Baselines strike back. In *Rep4NLP@ACL*, 2017. URL <https://api.semanticscholar.org/CorpusID:7557552>.
- J. M. Kanter and K. Veeramachaneni. Deep feature synthesis: Towards automating data science endeavors. In *2015 IEEE international conference on data science and advanced analytics (DSAA)*, pages 1–10. IEEE, 2015.

- G. Karypis and V. Kumar. Metis: A software package for partitioning unstructured graphs, partitioning meshes, and computing fill-reducing orderings of sparse matrices. 1997.
- A. Kochsiek, F. Niesel, and R. Gemulla. Start small, think big: On hyperparameter optimization for large-scale knowledge graph embeddings. In *Joint European Conference on Machine Learning and Knowledge Discovery in Databases*, pages 138–154. Springer, 2022.
- R. B. Lehoucq, D. C. Sorensen, and C. Yang. *ARPACK users’ guide: solution of large-scale eigenvalue problems with implicitly restarted Arnoldi methods*. SIAM, 1998.
- D. Lenat and E. Feigenbaum. On the thresholds of knowledge. *Artificial Intelligence: Critical Concepts*, 2:298, 2000.
- A. Lerer, L. Wu, J. Shen, T. Lacroix, L. Wehrstedt, A. Bose, and A. Peysakhovich. Pytorch-biggraph: A large scale graph embedding system. *Proceedings of Machine Learning and Systems*, 1:120–131, 2019.
- J. Leskovec, K. J. Lang, A. Dasgupta, and M. W. Mahoney. Community structure in large networks: Natural cluster sizes and the absence of large well-defined clusters. *Internet Mathematics*, 6(1):29–123, 2009.
- O. Levy and Y. Goldberg. Neural word embedding as implicit matrix factorization. *Advances in neural information processing systems*, 27, 2014.
- J. Liang, S. Gurukar, and S. Parthasarathy. Mile: A multi-level framework for scalable graph embedding. In *Proceedings of the International AAAI Conference on Web and Social Media*, volume 15, pages 361–372, 2021.
- F. Mahdisoltani, J. Biega, and F. Suchanek. Yago3: A knowledge base from multilingual wikipedias. In *7th biennial conference on innovative data systems research*. CIDR Conference, 2014.
- P. N. Mendes, M. Jakob, A. García-Silva, and C. Bizer. Dbpedia spotlight: shedding light on the web of documents. In *Proceedings of the 7th international conference on semantic systems*, pages 1–8, 2011.
- T. Mikolov, K. Chen, G. Corrado, and J. Dean. Efficient estimation of word representations in vector space. *arXiv preprint arXiv:1301.3781*, 2013a.
- T. Mikolov, I. Sutskever, K. Chen, G. S. Corrado, and J. Dean. Distributed representations of words and phrases and their compositionality. *Advances in neural information processing systems*, 26, 2013b.
- J. Mohoney, R. Waleffe, H. Xu, T. Rekatsinas, and S. Venkataraman. Marius: Learning massive graph embeddings on a single machine. In *15th {USENIX} Symposium on Operating Systems Design and Implementation ({OSDI} 21)*, pages 533–549, 2021.
- O. Mutlu, S. Ghose, J. Gómez-Luna, and R. Ausavarungnirun. A modern primer on processing in memory. In *Emerging computing: from devices to systems: looking beyond Moore and Von Neumann*, pages 171–243. Springer, 2022.
- M. E. Newman. Finding community structure in networks using the eigenvectors of matrices. *Physical review E*, 74(3):036104, 2006.
- F. Pedregosa, G. Varoquaux, A. Gramfort, V. Michel, B. Thirion, O. Grisel, M. Blondel, P. Prettenhofer, R. Weiss, V. Dubourg, et al. Scikit-learn: Machine learning in python. *the Journal of machine Learning research*, 12:2825–2830, 2011.
- T. Pellissier Tanon, G. Weikum, and F. Suchanek. Yago 4: A reason-able knowledge base. In *European Semantic Web Conference*, pages 583–596. Springer, 2020.
- B. Perozzi, R. Al-Rfou, and S. Skiena. Deepwalk: Online learning of social representations. In *Proceedings of the 20th ACM SIGKDD international conference on Knowledge discovery and data mining*, pages 701–710, 2014.
- F. Petroni, L. Querzoni, K. Daudjee, S. Kamali, and G. Iacoboni. Hdrf: Stream-based partitioning for power-law graphs. In *Proceedings of the 24th ACM international on conference on information and knowledge management*, pages 243–252, 2015.
- S. T. Piantadosi. Zipf’s word frequency law in natural language: A critical review and future directions. *Psychonomic bulletin & review*, 21:1112–1130, 2014.
- J. Qiu, Y. Dong, H. Ma, J. Li, K. Wang, and J. Tang. Network embedding as matrix factorization: Unifying deepwalk, line, pte, and node2vec. In *Proceedings of the eleventh ACM international conference on web search and data mining*, pages 459–467, 2018.

- U. N. Raghavan, R. Albert, and S. Kumara. Near linear time algorithm to detect community structures in large-scale networks. *Physical review E*, 76(3):036106, 2007.
- J. Reagle and L. Rhue. Gender bias in wikipedia and britannica. *International Journal of Communication*, 5:21, 2011.
- H. Ren, H. Dai, B. Dai, X. Chen, D. Zhou, J. Leskovec, and D. Schuurmans. Smore: Knowledge graph completion and multi-hop reasoning in massive knowledge graphs. In *Proceedings of the 28th ACM SIGKDD Conference on Knowledge Discovery and Data Mining*, pages 1472–1482, 2022.
- P. Ristoski and H. Paulheim. Rdf2vec: Rdf graph embeddings for data mining. In *The Semantic Web–ISWC 2016: 15th International Semantic Web Conference, Kobe, Japan, October 17–21, 2016, Proceedings, Part I 15*, pages 498–514. Springer, 2016.
- J. Robinson, R. Ranjan, W. Hu, K. Huang, J. Han, A. Dobles, M. Fey, J. E. Lenssen, Y. Yuan, Z. Zhang, et al. Relbench: A benchmark for deep learning on relational databases. *Advances in Neural Information Processing Systems*, 37:21330–21341, 2025.
- E. Rossi, H. Kenlay, M. I. Gorinova, B. P. Chamberlain, X. Dong, and M. M. Bronstein. On the unreasonable effectiveness of feature propagation in learning on graphs with missing node features. In *Learning on graphs conference*, pages 11–1. PMLR, 2022.
- M. Rosvall and C. T. Bergstrom. Maps of random walks on complex networks reveal community structure. *Proceedings of the national academy of sciences*, 105(4):1118–1123, 2008.
- D. Ruffinelli and R. Gemulla. Beyond link prediction: On pre-training knowledge graph embeddings. In *Proceedings of the 9th Workshop on Representation Learning for NLP (RepL4NLP-2024)*, pages 136–162, 2024.
- D. Ruffinelli, S. Broscheit, and R. Gemulla. You can teach an old dog new tricks! on training knowledge graph embeddings. In *International Conference on Learning Representations*, 2020. URL <https://openreview.net/forum?id=BkxSmlBFvr>.
- C. Ruiz, H. Ren, K. Huang, and J. Leskovec. High dimensional, tabular deep learning with an auxiliary knowledge graph. *Advances in Neural Information Processing Systems*, 36, 2024.
- J. Shi and J. Malik. Normalized cuts and image segmentation. *IEEE Transactions on pattern analysis and machine intelligence*, 22(8):888–905, 2000.
- R. Speer, J. Chin, and C. Havasi. Conceptnet 5.5: An open multilingual graph of general knowledge. In *Proceedings of the AAAI conference on artificial intelligence*, volume 31, 2017.
- I. Stanton and G. Kliot. Streaming graph partitioning for large distributed graphs. In *Proceedings of the 18th ACM SIGKDD international conference on Knowledge discovery and data mining*, pages 1222–1230, 2012.
- F. M. Suchanek, M. Alam, T. Bonald, L. Chen, P.-H. Paris, and J. Soria. Yago 4.5: A large and clean knowledge base with a rich taxonomy. In *Proceedings of the 47th International ACM SIGIR Conference on Research and Development in Information Retrieval*, pages 131–140, 2024.
- D. Sullivan. A reintroduction to our knowledge graph and knowledge panels. <https://blog.google/products/search/about-knowledge-graph-and-knowledge-panels/>, 2020. Accessed: 2025-01-26.
- Z. Sun, Z.-H. Deng, J.-Y. Nie, and J. Tang. Rotate: Knowledge graph embedding by relational rotation in complex space. In *International Conference on Learning Representations*, 2019. URL <https://openreview.net/forum?id=HkgEQnRqYQ>.
- P. Tabacof and L. Costabello. Probability calibration for knowledge graph embedding models. In *International Conference on Learning Representations*, 2020. URL <https://openreview.net/forum?id=S1g8K1BFwS>.
- J. Tang, M. Qu, M. Wang, M. Zhang, J. Yan, and Q. Mei. Line: Large-scale information network embedding. In *Proceedings of the 24th international conference on world wide web*, pages 1067–1077, 2015.
- M. A. Terpilowski. scikit-posthocs: Pairwise multiple comparison tests in python. *Journal of Open Source Software*, 4(36):1169, 2019.
- V. A. Traag, L. Waltman, and N. J. Van Eck. From louvain to leiden: guaranteeing well-connected communities. *Scientific reports*, 9(1):5233, 2019.

- T. Trouillon, J. Welbl, S. Riedel, É. Gaussier, and G. Bouchard. Complex embeddings for simple link prediction. In *International conference on machine learning*, pages 2071–2080. PMLR, 2016.
- C. Tsourakakis, C. Gkantsidis, B. Radunovic, and M. Vojnovic. Fennel: Streaming graph partitioning for massive scale graphs. In *Proceedings of the 7th ACM international conference on Web search and data mining*, pages 333–342, 2014.
- G. M. Van de Ven, T. Tuytelaars, and A. S. Tolias. Three types of incremental learning. *Nature Machine Intelligence*, 4:1185–1197, 2022.
- S. Vashishth, S. Sanyal, V. Nitin, and P. Talukdar. Composition-based multi-relational graph convolutional networks. In *International Conference on Learning Representations*, 2020. URL https://openreview.net/forum?id=By1A_C4tPr.
- L. Vogel, J.-M. Bodensohn, and C. Binnig. Wikidbs: A large-scale corpus of relational databases from wikidata. *Advances in Neural Information Processing Systems*, 37:41186–41201, 2024.
- D. Vrandečić and M. Krötzsch. Wikidata: a free collaborative knowledgebase. *Communications of the ACM*, 57(10):78–85, 2014.
- R. Waleffe, J. Mohoney, T. Rekatsinas, and S. Venkataraman. Mariusgnn: Resource-efficient out-of-core training of graph neural networks. In *Proceedings of the Eighteenth European Conference on Computer Systems*, pages 144–161, 2023.
- H. Wang, S. Dai, W. Su, H. Zhong, Z. Fang, Z. Huang, S. Feng, Z. Chen, Y. Sun, and D. Yu. Simple and effective relation-based embedding propagation for knowledge representation learning. In *IJCAI-ECAI*, 2022.
- Q. Wang, Z. Mao, B. Wang, and L. Guo. Knowledge graph embedding: A survey of approaches and applications. *IEEE transactions on knowledge and data engineering*, 29(12):2724–2743, 2017.
- Wikimedia. Wikidata growth. https://wikitech.wikimedia.org/wiki/WMD/WMDE/Wikidata/Growth#Number_of_Entities_by_type. [Online; accessed in January 2025].
- C. Xie, L. Yan, W.-J. Li, and Z. Zhang. Distributed power-law graph computing: Theoretical and empirical analysis. *Advances in neural information processing systems*, 27, 2014.
- B. Yang, W.-t. Yih, X. He, J. Gao, and L. Deng. Embedding entities and relations for learning and inference in knowledge bases. In *Proceedings of the 3rd International Conference on Learning Representations (ICLR)*, 2015. URL <https://arxiv.org/abs/1412.6575>.
- H. Zeng, H. Zhou, A. Srivastava, R. Kannan, and V. Prasanna. GraphSAINT: Graph sampling based inductive learning method. In *International Conference on Learning Representations*, 2020. URL <https://openreview.net/forum?id=BJe8pkHFwS>.
- S. Zhang, Y. Tay, L. Yao, and Q. Liu. Quaternion knowledge graph embeddings. *Advances in neural information processing systems*, 32, 2019.
- C. Zheng, G. Jiang, X. Yan, P. Yin, Q. Zhou, and J. Cheng. Ge2: A general and efficient knowledge graph embedding learning system. *Proceedings of the ACM on Management of Data*, 2(3):1–27, 2024.
- D. Zheng, X. Song, C. Ma, Z. Tan, Z. Ye, J. Dong, H. Xiong, Z. Zhang, and G. Karypis. Dgl-ke: Training knowledge graph embeddings at scale. In *Proceedings of the 43rd international ACM SIGIR conference on research and development in information retrieval*, pages 739–748, 2020.
- Z. Zhu, S. Xu, J. Tang, and M. Qu. Graphvite: A high-performance cpu-gpu hybrid system for node embedding. In *The World Wide Web Conference*, pages 2494–2504, 2019.

Appendix - Table of Contents

A Datasets	16
A.1 Statistics on knowledge graph datasets	16
A.2 Downstream tables	16
A.3 Entity coverage of downstream tables	17
B Evaluation methodology	19
B.1 Downstream tasks	19
B.2 Knowledge graph completion	22
B.3 Experimental setup	23
C Additional evaluation of SEPAL	23
C.1 Table-level downstream results on real-world tables	23
C.2 Table-level downstream results on WikiDBs tables	23
C.3 SEPAL combined with more embedding models	23
C.4 Evaluation on knowledge graph completion	25
D Theoretical analysis	26
D.1 Analysis of SEPAL’s dynamic and analogies to eigenvalue problems	27
D.2 Formal proof of Proposition 4.1	28
E Presentation and analysis of BLOCS	29
E.1 Prior work on graph partitioning	29
E.2 Detailed algorithm and pseudocode	30
E.3 Benchmarking BLOCS against partitioning methods	32
E.4 Effect of BLOCS’ stopping diffusion threshold	34
E.5 How distant from the core are the outer entities?	34
F Further analysis of SEPAL	34
F.1 Execution time breakdown	34
F.2 SEPAL’s hyperparameters	36
F.3 Ablation study: SEPAL without BLOCS	39
F.4 Speedup over base embedding model	40
G Discussion	41
G.1 Comparison between SEPAL and NodePiece	41
G.2 Communication costs of SEPAL	42
G.3 Broader impacts	43

Table 2: Additional statistics on the knowledge graph datasets used. MSPL stands for Mean Shortest Path Length. The LCC column gives the percentage of entities of the graph that are in the largest connected component.

	Maximum degree	Average degree	MSPL	Diameter	Density	LCC
Mini YAGO3	65 711	12.6	3.3	11	1e-4	99.98%
YAGO3	934 599	4.0	4.2	23	2e-6	97.6%
YAGO4.5	6 434 121	4.5	5.0	502	1e-7	99.7%
YAGO4.5+T	6 434 122	5.0	4.0	5	1e-7	100%
YAGO4	8 606 980	12.9	4.5	28	3e-7	99.0%
YAGO4+T	32 127 569	9.4	3.4	6	1e-7	100%
Freebase	10 754 238	4.9	4.7	100	6e-8	99.1%
WikiKG90Mv2	37 254 176	12.8	3.6	98	1e-7	100.0%

Table 3: Number of rows in the downstream tables.

	US elections	Housing prices	US accidents	Movie revenues
Number of rows	13 656	22 250	20 332	7 398

A Datasets

A.1 Statistics on knowledge graph datasets

More statistics on the knowledge graph datasets are given in Table 2. Maximum and average degree figures highlight the scale-free nature of real-world knowledge graphs. The values for mean shortest path length (MSPL) and diameter (the diameter is the longest shortest path) are provided for the largest connected component (LCC). They are remarkably small, given the number of entities in the graphs. Contrary to other datasets, YAGO4.5, Freebase, and WikiKG90Mv2 contain ‘long chains’ of nodes, which account for their larger diameters.

The density D is the ratio between the number of edges $|E|$ and the maximum possible number of edges:

$$D = \frac{|E|}{|\mathcal{V}|(|\mathcal{V}| - 1)}$$

where $|\mathcal{V}|$ denotes the number of nodes.

The LCC statistics show that for each knowledge graph, the largest connected component regroups almost all the entities.

A.2 Downstream tables

Real-world tables We use 4 real-world downstream tasks adapted from Cvetkov-Iliev et al. (2023) who also investigate knowledge-graph embeddings to facilitate machine learning. The specific target values predicted for each dataset are the following:

US elections: predict the number of votes per party in US counties;

Housing prices: predict the average housing price in US cities;

US accidents: predict the number of accidents in US cities;

Movie revenues: predict the box-office revenues of movies.

For each table, a log transformation is applied to the target values as a preprocessing step. Table 3 contains the sizes of these real-world downstream tables.

WikiDBs tables WikiDBs contains 100,000 databases (collections of related tables), which altogether include 1,610,907 tables. We extracted 42 of those tables to evaluate embeddings. Here we describe the procedure used for table selection and processing.

Table 4: **Regression tables from WikiDBs.** The ‘DB number’ is the number of the database in WikiDBs from which the table was taken. Among these 16 regression tables, 2 are used for validation, and 14 for test.

Table name	DB number	Value to predict	N_{rows}	Set
Historical Figures	62 826	Birth date	3 000	Val
Geopolitical Regions	66 610	Land area	2 324	Val
Eclipsing Binary Star Instances	3 977	Apparent magnitude	3 000	Test
Research Article Citations	14 012	Publication date	3 000	Test
Drawings Catalog	14 976	Artwork height	3 000	Test
Municipal District Capitals	19 664	Population count	2 846	Test
Twinned Cities	28 146	Population	1 194	Test
Ukrainian Village Instances	28 324	Elevation (meters)	3 000	Test
Dissolved Municipality Records	46 159	Dissolution date	3 000	Test
Research Articles	53 353	Publication date	3 000	Test
Territorial Entities	82 939	Population count	3 000	Test
Artworks Inventory	88 197	Artwork width	3 000	Test
Business Entity Locations	89 039	Population count	3 000	Test
WWI Personnel Profiles	89 439	Birth date	3 000	Test
Registered Ships	90 930	Gross tonnage	3 000	Test
Poet Profiles	94 062	Death date	3 000	Test

Table selection: Most of the WikiDBs tables are very small –typically a few dozen samples– so our first filtering criterion was the table size, which must be large enough to enable fitting an estimator. Therefore, we randomly sampled 100 tables from WikiDBs with sufficient sizes ($N_{\text{rows}} > 1,000$). Then we looked at each sampled table individually and kept those that could be used to define a relevant machine learning task (either regression or classification). We ended up with 16 regression tasks and 26 classification tasks.

Table processing: We removed rows with missing values, and reduced the size of large tables to keep evaluation tractable. For regression tables, we simply sampled 3,000 rows randomly (if the table had more than 3,000). We applied a log transformation to the target values to remove the skewness of their distributions. Before that, dates were converted into floats (by first converting them to fractional years, and then applying the transform $t \mapsto 2025 - t$). For classification tables, to reduce the dataset sizes while preserving both class diversity and balance, we downsampled the tables with the following procedure:

1. Class filtering: we set a threshold $r = \min(50, 0.9N_2)$, where N_2 is the cardinality of the second most populated class, and retained only the classes with more than r occurrences.
2. Limit number of classes: if more than 30 classes remained after filtering, only the 30 most frequent were kept.
3. Downsampling: if the resulting table contained more than 3,000 rows, we sampled rows such that: (a) if $r \cdot N_{\text{classes}} \leq 3,000$, at least r rows were sampled per class, (b) if $r \cdot N_{\text{classes}} > 3,000$, we sampled an approximately equal number of rows per class, fitting within the 3,000-row limit.

The specifications of the 42 tables extracted are given in Table 4 and Table 5.

A.3 Entity coverage of downstream tables

Entity coverage We define the coverage of table T by knowledge graph K as the proportion of downstream entities in T that are described in K . Figure 4 gives the empirically measured coverage of the 46 downstream tables by the 8 different knowledge graphs used in our experimental study. It shows that larger and more recent knowledge graphs yield greater coverage.

Entity matching Leveraging knowledge-graph embeddings to enrich a downstream tabular prediction task requires mapping the table entries to entities of the knowledge graph. We call this process *entity matching*.

For the 4 real-world tables, we performed the entity matching ‘semi-automatically’, following Cvetkov-Iliev et al. (2023). The entries of these tables are well formatted and a small set of simple rules is

SCALABLE EMBEDDING FOR DOWNSTREAM MACHINE LEARNING

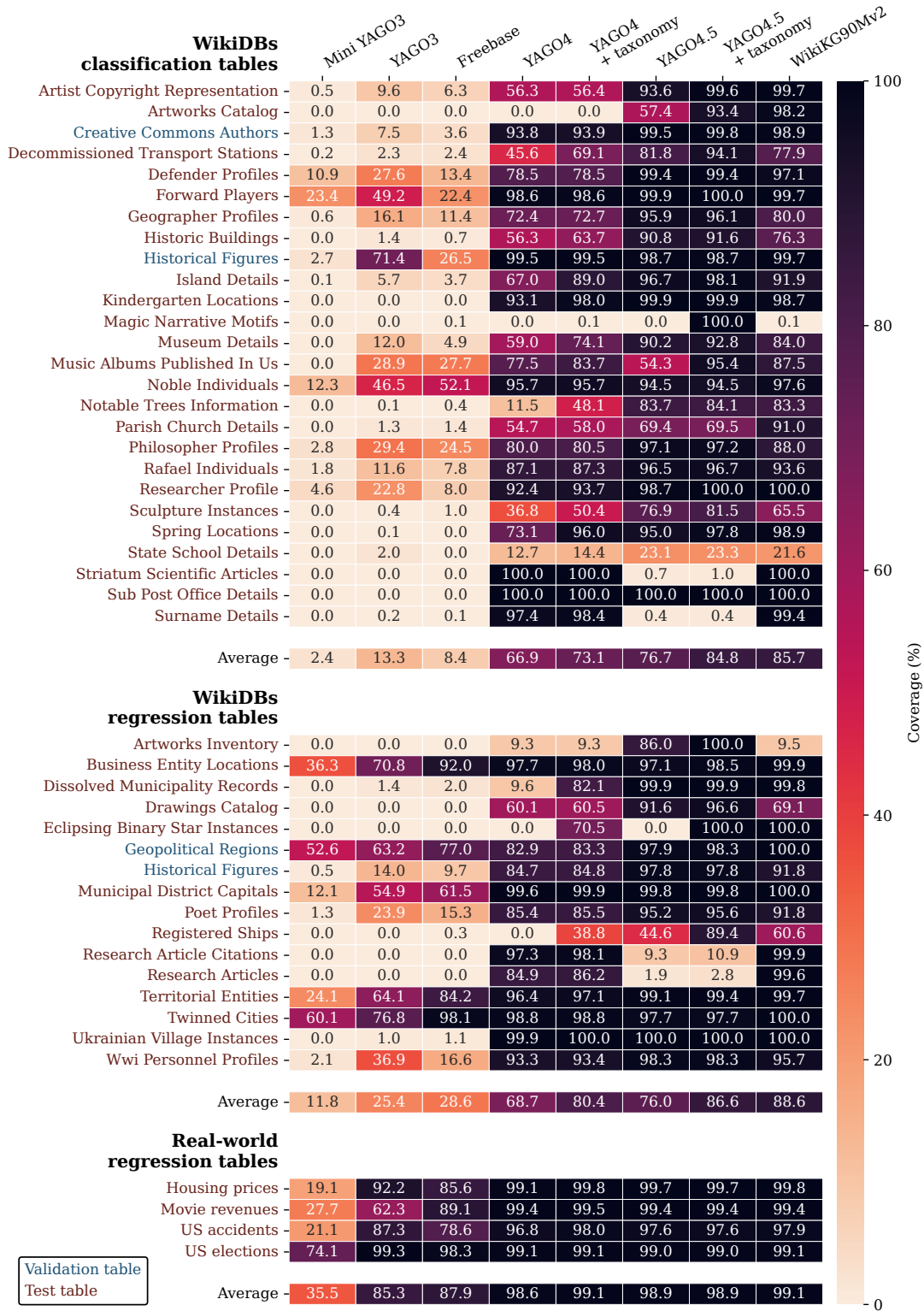


Figure 4: **Entity coverage of downstream tables.** Over the 46 downstream tables 4 are used for validation (in blue), and 42 are used for test (in maroon).

Table 5: **Classification tables from WikiDBs.** The ‘DB number’ is the number of the database in WikiDBs from which the table was taken. Among these 26 classification tables, 2 are used for validation, and 24 for test.

Table name	DB number	Class to predict	N _{rows}	N _{classes}	Set
Creative Commons Authors	9 510	Gender	2 999	2	Val
Historical Figures	73 376	Profession	1 044	5	Val
Historic Buildings	473	Country	2 985	30	Test
Striatum Scientific Articles	2 053	Journal name	2 986	30	Test
Researcher Profile	7 136	Affiliated institution	237	7	Test
Decommissioned Transport Stations	7 310	Country	2 983	30	Test
Artist Copyright Representation	7 900	Artist occupation	2 986	27	Test
Forward Players	15 542	Team	2 985	30	Test
Rafael Individuals	29 832	Nationality	2 966	12	Test
Artworks Catalog	30 417	Artwork type	2 991	17	Test
Magic Narrative Motifs	36 100	Cultural origin	2 993	12	Test
Geographer Profiles	42 562	Language	2 992	14	Test
Surname Details	47 746	Language	1 420	5	Test
Sculpture Instances	56 474	Material used	2 985	30	Test
Spring Locations	63 797	Country	2 981	30	Test
Noble Individuals	64 477	Role	2 987	30	Test
Defender Profiles	65 102	Defender position	2 998	5	Test
Kindergarten Locations	66 643	Country	2 998	4	Test
Sub Post Office Details	67 195	Administrative territory	2 986	30	Test
State School Details	70 780	Country	2 995	12	Test
Notable Trees Information	70 942	Tree species	2 992	19	Test
Parish Church Details	87 283	Country	2 993	15	Test
Museum Details	90 741	Country	2 986	30	Test
Island Details	92 415	Country	2 986	30	Test
Philosopher Profiles	97 229	Language	2 985	29	Test
Music Albums Published in the US	97 297	Music Genre	2 984	30	Test

sufficient to match the vast majority of entities. Human supervision was required for some cases of homonymy, for instance.

For the WikiDBs tables, we used the Wikidata Q identifiers (QIDs) included in the WikiDBs dataset to straightforwardly match the entities to WikiKG90Mv2¹, YAGO4, and YAGO4.5, which all provide the QIDs for every entity. YAGO4 also offers a mapping to the Freebase entities, which we used to match the Freebase entities to the WikiDBs tables. Additionally, both YAGO3 and YAGO4 provide mappings to DBpedia, which enabled us to obtain the matching for YAGO3.

B Evaluation methodology

B.1 Downstream tasks

Setting For each dataset, we use scikit-learn’s Histogram-based Gradient Boosting Regression (*resp.* Classification) Tree (Pedregosa et al., 2011) as regression (*resp.* classification) estimator to predict the target value. The embeddings are the only features fed to the estimator, except for the US elections dataset for which we also include the political party. For embedding models outputting complex embeddings, such as RotatE, we simply concatenate real and imaginary parts before feeding them to the estimator.

The rows of the tables corresponding to entities not found in the knowledge graph are filled with NaNs as features for the estimator. This enables to compare the scores between different knowledge graphs (see Figure 2 and Figure 3) of different sizes to see the benefits obtained from embedding larger graphs, with better coverage of downstream entities (Figure 4).

¹Entity mapping for WikiKG90Mv2 is provided [here](#).

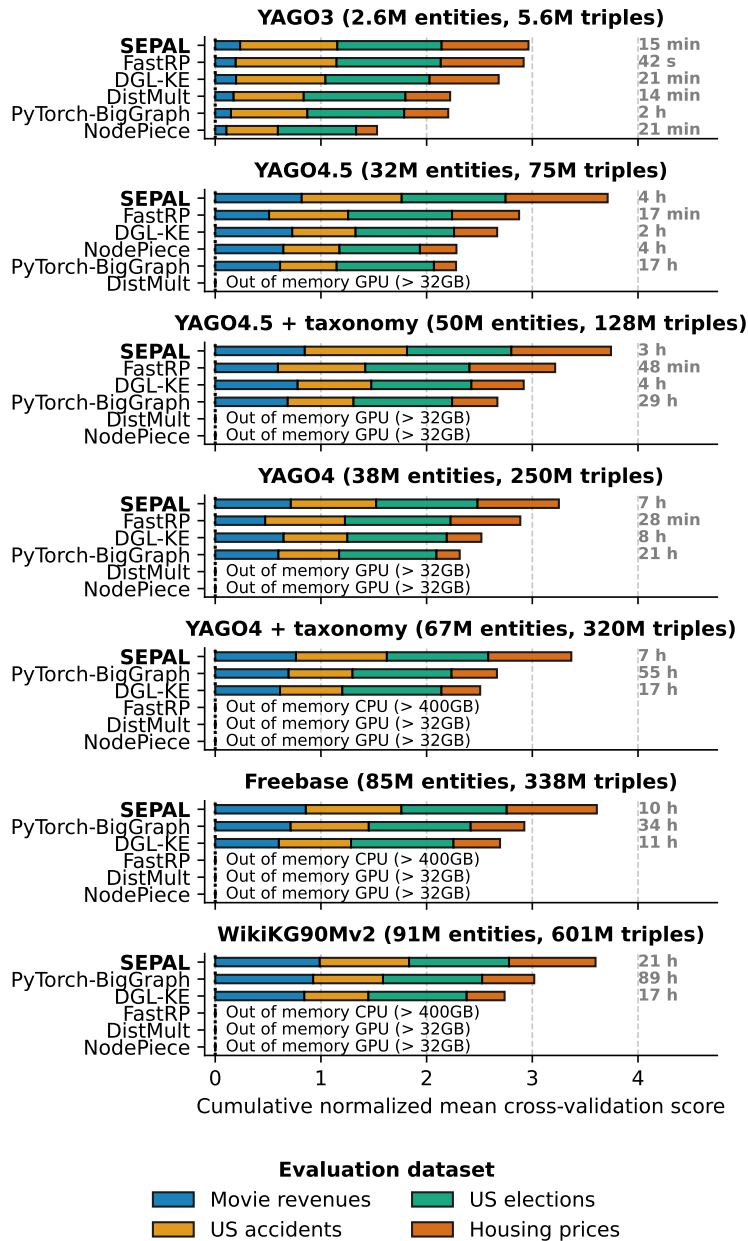


Figure 5: **Detailed results on real-world tables.** The "Cumulative normalized mean cross-validation score" reported is obtained by summing the normalized mean cross-validation scores. For an evaluation dataset, 1 corresponds to the best R2 score across all models; as there are 4 evaluation datasets, the highest possible score for a model is 4 (getting a score of 4 means that the model beats every model on every evaluation dataset). SEPAL, PyTorch-BigGraph, DGL-KE, and NodePiece use DistMult as base model. Embedding computation times are provided on the right-hand side of the figure. Figure 7 extends this figure with other embedding models.

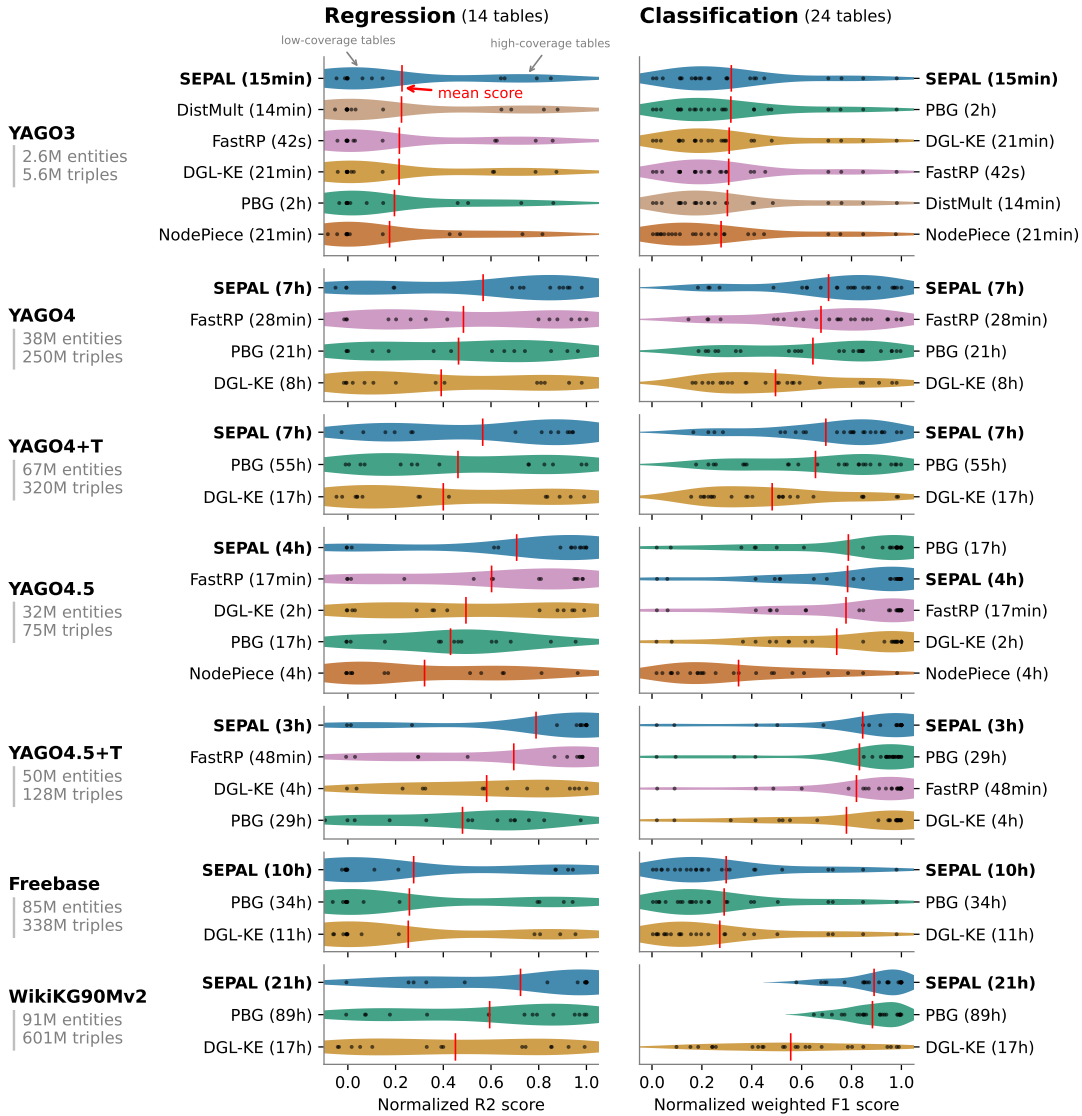


Figure 6: **Detailed results on WikiDBs tables.** Each black dot represents a downstream table. Red vertical lines indicate the mean score over all the tables. The methods appear in decreasing order of average score.

Metrics The metric used for regression is the R2 score, defined as:

$$R^2 = 1 - \frac{\sum_{i=1}^N (y_i - \hat{y}_i)^2}{\sum_{i=1}^N (y_i - \bar{y})^2}$$

where N is the number of samples (rows) in the target table, y_i is the target value of sample i , \hat{y}_i is the value predicted by the estimator, and \bar{y} is the mean value of the target variable.

For classification, we use the weighted F1 score, defined as:

$$F1_{\text{weighted}} = \sum_{i=1}^K \frac{n_i}{N} \cdot F1_i$$

where K is the number of classes, n_i is the number of true instances for class i , $N = \sum_{i=1}^K n_i$ is the total number of samples, and $F1_i$ is the F1 score for class i .

To get the "Mean score (normalized)" reported on Figure 2 and Figure 3, we proceed as follows:

1. **Mean cross-validation score:** for each model² and evaluation table, the scores (R2 or weighted F1, depending on the task) are averaged over 5 repeats of 5-fold cross-validations.
2. **Normalized:** for each evaluation table, we divide the scores of the different models by the score of the best-performing model on this table. This makes the scores more comparable between the different evaluation tables.
3. **Average:** for each model, we average its scores across every evaluation table. The highest possible score for a model is 1. Getting a score of 1 means that the model beats every other model on every evaluation table.

Validation/test split and hyperparameter tuning We use 4 of the 42 WikiDBs tables as validation data—2 for regression and 2 for classification tasks (see Figure 4). The remaining 38 WikiDBs tables, along with the 4 real-world tables, are used exclusively for testing.

The validation tables are used to tune hyperparameters and select the best-performing configuration for each method and each knowledge graph. Unless otherwise specified, all reported results are obtained on the test tables using these optimized configurations.

B.2 Knowledge graph completion

We detail our experimental setup for the link prediction task:

Setting: We evaluate models under the transductive setting: the missing links to be predicted connect entities already seen in the train graph. The task is to predict the tail entity of a triple, given its head and relation.

Stratification: We randomly split each dataset into training (90%), validation (5%), and test (5%) subsets of triples. During stratification, we ensure that the train graph remains connected by moving as few triples as required from the validation/test sets to the training set.

Sampling: Given the size of our datasets, sampling is required to keep link prediction tractable. For each evaluation triple, we sample 10,000 negative entities uniformly to produce 10,000 candidate negative triples by corrupting the positive.

Filtering: For tractability reasons, we report unfiltered results: we do not remove triples already existing in the dataset (which may score higher than the test triple) from the candidates.

Ranking: If several triples have the same score, we report realistic ranks (i.e., the expected ranking value over all permutations respecting the sort order; see PyKEEN documentation (Ali et al., 2021b)).

Metrics: We use three standard metrics for link prediction: the mean reciprocal rank (MRR), hits at k (for $k \in \{1, 10, 50\}$) and mean rank (MR). Given the rankings r_1, \dots, r_n of the n evaluation

²We define "model" as the combination of a method (e.g. DistMult, DGL-KE, etc.) and a knowledge graph on which it is trained.

(validation or test) triples:

$$\text{MRR} = \frac{1}{n} \sum_{i=1}^n \frac{1}{r_i}, \quad \text{Hits}@k = \frac{1}{n} \sum_{i=1}^n 1_{r_i \leq k}, \quad \text{MR} = \frac{1}{n} \sum_{i=1}^n r_i.$$

B.3 Experimental setup

Baseline implementations In our empirical study, we compare SEPAL to DistMult, NodePiece, PBG, DGL-KE, and FastRP. We use the PyKEEN (Ali et al., 2021b) implementation for DistMult and NodePiece, and the implementations provided by the authors for the others. PBG was trained on 20 CPU nodes, and DGL-KE was allocated 20 CPU nodes and 3 GPUs; both methods were run on a single machine. The version of NodePiece we use for datasets larger than Mini YAGO3 is the ablated version, where nodes are tokenized only from their relational context (otherwise, the method does not scale on our hardware). For PBG, DGL-KE, NodePiece, and FastRP we used the hyperparameters provided by the authors for datasets of similar sizes. SEPAL and DistMult’s hyperparameters were tuned on the validation sets presented in Appendix B.1 and Appendix B.2.

For all the baseline clustering algorithms, we used the implementations from the igraph package (Csardi, 2013) except for METIS, HDRF and Spectral Clustering. For METIS, we used the torch-sparse implementation, for Spectral Clustering, the scikit-learn (Pedregosa et al., 2011) implementation, and for HDRF, we used the C++ implementation from this repository.

Computer resources For PBG and FastRP, experiments were carried out on a machine with 48 cores and 504 GB of RAM. DistMult, DGL-KE, NodePiece, and SEPAL were trained on Nvidia V100 GPUs with 32 GB of memory, and 20 CPU nodes with 252 GB of RAM. The clustering benchmark was run on a machine with 88 CPU nodes and 504 GB of RAM.

C Additional evaluation of SEPAL

C.1 Table-level downstream results on real-world tables

Figure 5 shows the detailed prediction performance on the downstream tasks. SEPAL not only scales well to very large graphs (computing times markedly smaller than Pytorch-BigGraph), but also creates more valuable node features for downstream tasks.

C.2 Table-level downstream results on WikiDBs tables

Figure 6 shows the detailed downstream tasks results for the WikiDBs test tables. For regression, SEPAL is the best performer on average for all of the 7 knowledge graphs. For classification, SEPAL is the best method on 6 of 7 knowledge graphs (narrowly beaten by PBG on YAGO4.5). Interestingly, FastRP, despite being very simple and not even accounting for relations, is a strong performer and beats more sophisticated methods like PBG and DGL-KE on many tasks. This is consistent with our *queriability* analysis in section 4 concluding that global methods, such as FastRP and SEPAL, are more suitable for downstream tasks, than local methods (such as PBG and DGL-KE).

For some knowledge graphs (especially Freebase and YAGO3), we can see two modes in the scores distribution, corresponding to the tables with low and high coverages (Figure 4).

C.3 SEPAL combined with more embedding models

Figure 7 extends the results of Figure 5 by adding TransE and RotatE, alone and combined with SEPAL, as well as ablation studies results of SEPAL combined with METIS or ablated from BLOCS. These results show that SEPAL systematically improves upon its base model, whether it be DistMult RotatE or TransE. For a fair comparison, we ran RotatE with embedding dimension $d = 50$, as it outputs complex embeddings having twice as many parameters. For other models, we use $d = 100$.

SCALABLE EMBEDDING FOR DOWNSTREAM MACHINE LEARNING

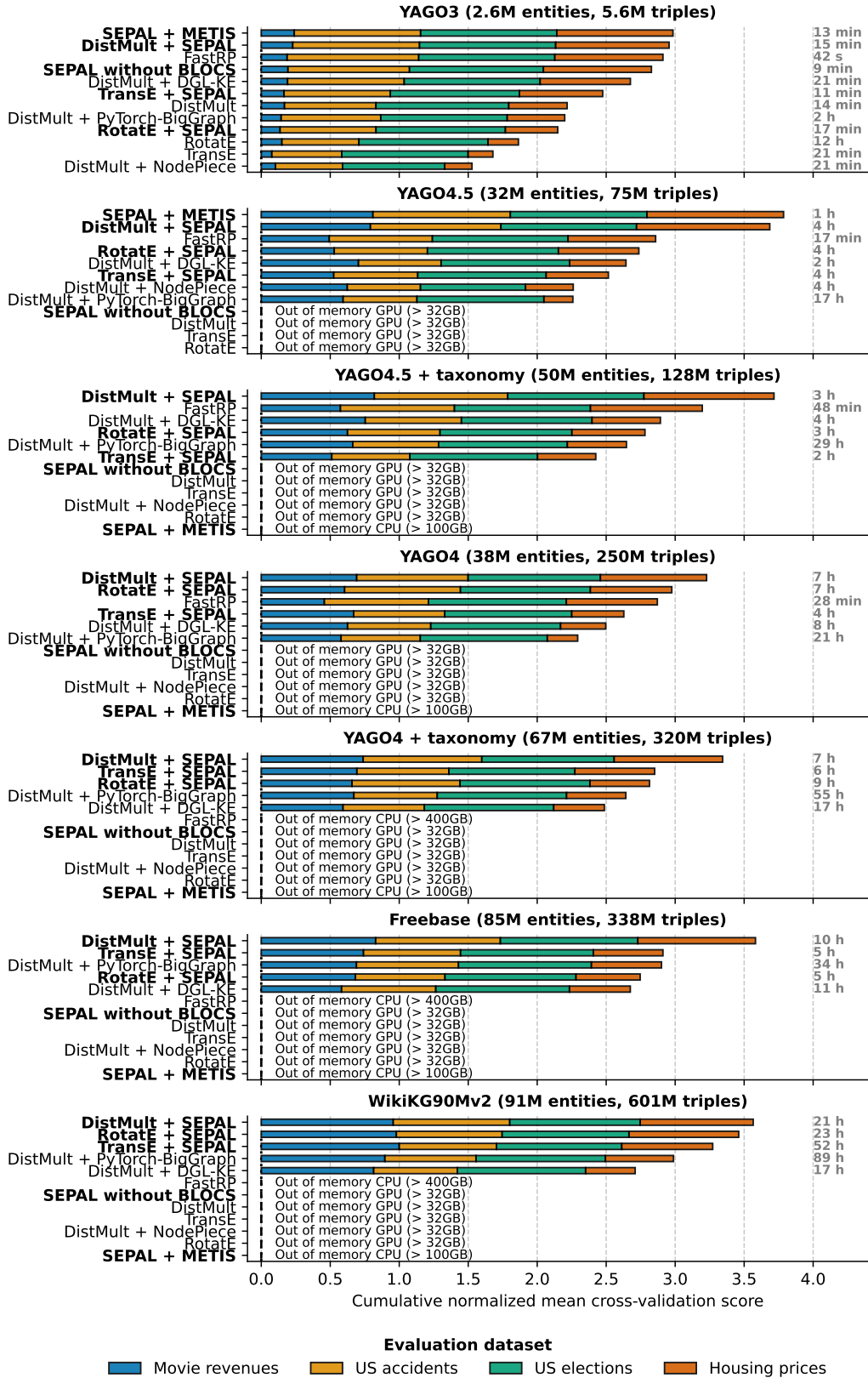
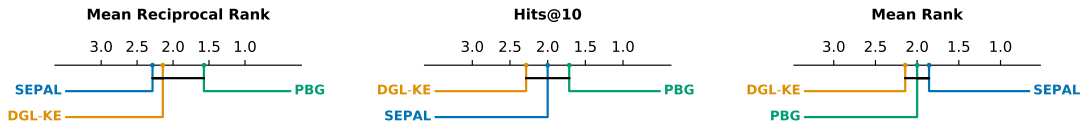


Figure 7: Performance on real-world downstream tables.

Table 6: Results for link prediction. Best in bold, second underlined.

	YAGO3	YAGO4.5	YAGO4.5+T	YAGO4	YAGO4+T	Freebase	WikiKG90Mv2	Average
a. MRR								
DistMult	0.8049	-	-	-	-	-	-	-
NodePiece	0.2596	0.4456	-	-	-	-	-	-
PBG	0.5581	<u>0.5539</u>	<u>0.5688</u>	0.6406	0.6224	0.7389	0.6325	0.6165
DGL-KE	<u>0.7284</u>	0.6200	0.6469	0.2372	0.2570	0.3017	0.3202	0.4445
SEPAL	0.6501	0.5537	0.5646	<u>0.4726</u>	<u>0.477</u>	<u>0.5378</u>	<u>0.5291</u>	<u>0.5407</u>
b. Hits@1								
DistMult	0.7400	-	-	-	-	-	-	-
NodePiece	0.1735	0.3449	-	-	-	-	-	-
PBG	0.5000	0.4939	<u>0.4977</u>	0.5494	0.5416	0.7015	0.5568	0.5487
DGL-KE	<u>0.6663</u>	0.5511	0.5733	0.1642	0.1892	0.2498	0.2416	0.3765
SEPAL	0.5412	0.4913	0.4922	<u>0.3746</u>	<u>0.3755</u>	<u>0.4824</u>	<u>0.4502</u>	<u>0.4582</u>
c. Hits@10								
DistMult	0.9059	-	-	-	-	-	-	-
NodePiece	0.4388	0.6379	-	-	-	-	-	-
PBG	0.6562	0.6642	<u>0.7021</u>	0.803	0.7662	0.8053	0.7693	0.7380
DGL-KE	0.8293	0.7446	0.7821	0.3786	0.3842	0.3964	0.4694	0.5692
SEPAL	<u>0.8394</u>	<u>0.6650</u>	0.6871	<u>0.6573</u>	<u>0.6778</u>	<u>0.6398</u>	<u>0.6739</u>	<u>0.6915</u>
d. Hits@50								
DistMult	0.9504	-	-	-	-	-	-	-
NodePiece	0.7358	<u>0.8112</u>	-	-	-	-	-	-
PBG	0.7259	0.7734	<u>0.8136</u>	0.8891	0.8514	0.8541	0.8531	0.8229
DGL-KE	0.8873	0.8171	0.8748	0.6037	0.5968	0.5547	0.654	0.7126
SEPAL	<u>0.9204</u>	0.7698	0.7786	<u>0.7661</u>	<u>0.8068</u>	<u>0.7476</u>	<u>0.7805</u>	<u>0.7957</u>
e. MR								
DistMult	64.19	-	-	-	-	-	-	-
NodePiece	154.7	263.2	-	-	-	-	-	-
PBG	820.9	408.0	300.3	117.1	203.5	<u>243.4</u>	<u>227.3</u>	331.5
DGL-KE	187.7	624.1	<u>219.9</u>	<u>224.9</u>	<u>271.5</u>	227.0	186	277.3
SEPAL	<u>95.87</u>	<u>270.4</u>	206.0	553.0	363.2	357.3	365.5	<u>315.9</u>


 Figure 8: **Critical difference diagrams on link prediction metrics.** Statistical tests show no significant difference between methods at significance level $\alpha = 0.05$.

C.4 Evaluation on knowledge graph completion

Link prediction results

Table 6 provides the link prediction results for the different metrics. It shows that, depending on the dataset, SEPAL is competitive with existing methods (DGL-KE, PBG) or not. However, none of the methods is consistently better than the others for all datasets. Following the analysis in section 4, these results are expected given that SEPAL does not enforce local contrast between positive and negative triples through contrastive learning with negative sampling, like other KGE methods do, but rather focuses on global consistency of the embeddings. Link prediction is, by essence, a local task, asking

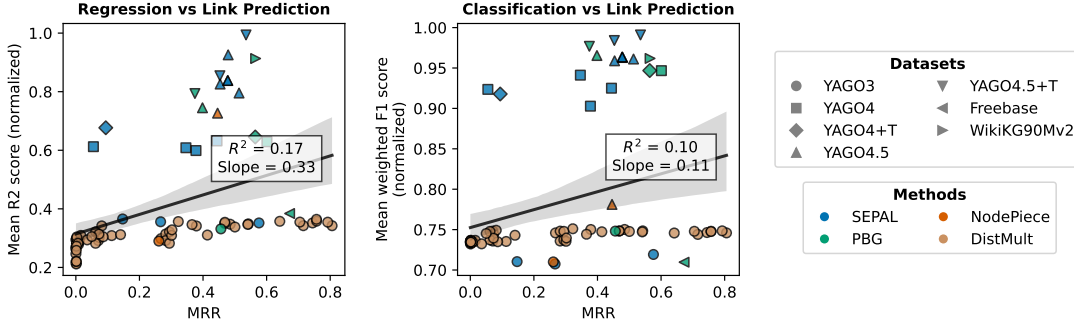


Figure 9: **Downstream task performance against link prediction performance**, on validation sets. Linear regression, with a 95% confidence interval. We plot the performance of models that share the same hyperparameters on the train graph (used for link prediction) and the full graph (used for downstream tasks).

to discriminate efficiently between positives and negatives. For this purpose, it seems that the negative sampling, absent from SEPAL’s propagation, plays a crucial role.

Nevertheless, Figure 8 shows that a Friedman test followed by Conover’s post-hoc analysis (Conover and Iman, 1979; Conover, 1999) reveal no statistically significant differences (at significance level $\alpha = 0.05$) among the three methods that scale to all the knowledge graphs (SEPAL, PBG, and DGL-KE), as indicated by the critical difference diagrams where all methods are connected by a black line.

From a hyperparameter perspective, contrary to downstream tasks, the hybrid core selection strategy (with both node and relation sampling) yields better results than its simpler degree-based counterpart. This highlights different trade-offs between downstream tasks and link prediction. For link prediction, good relational coverage seems to count most, whereas for downstream tasks, the core density matters most (Figure 20).

Downstream and link prediction performance weakly correlate

Figure 9 shows that embeddings performing well on downstream tasks do not necessarily perform well on link prediction, and vice versa. There is only a small positive correlation between these two performances: $R^2 \sim 0.1$.

D Theoretical analysis

Notations We use the following notations:

- $\Theta^{(t)} \in \mathbb{R}^{n \times d}$ is the embedding matrix at step t , where each row is the embedding of an entity. Without loss of generality, we assume that the entities are ordered core first, then outer, so we can write $\Theta^{(t)} = \begin{bmatrix} \Theta_c \\ \Theta_o^{(t)} \end{bmatrix}$ with $\Theta_c \in \mathbb{R}^{n_c \times d}$ the embedding matrix of core (fixed) entities, and $\Theta_o^{(t)} \in \mathbb{R}^{n_o \times d}$ the embedding matrix of outer (updated) entities at step t . n_c and n_o denote the number of core and outer entities, respectively, and $n_c + n_o = n$ is the total number of entities.
- $w_r \in \mathbb{R}^d$: embedding of relation $r \in \mathcal{R}$ (fixed).
- $\mathbf{x}^{(t)} = \text{vec}(\Theta^{(t)}) = \begin{bmatrix} \Theta_{1,1}^{(t)}, \dots, \Theta_{n,1}^{(t)}, \Theta_{1,2}^{(t)}, \dots, \Theta_{n,2}^{(t)}, \dots, \Theta_{1,d}^{(t)}, \dots, \Theta_{n,d}^{(t)} \end{bmatrix}^\top \in \mathbb{R}^{nd}$: vectorization of the embedding matrix.
- $\mathbf{P} \in \mathbb{R}^{nd \times nd}$: global linear propagation matrix.
- $\mathbf{Q} \in \mathbb{R}^{nd \times nd}$: permutation matrix to reorder \mathbf{x} into core and outer blocks.
- $\mathbf{y}^{(t)} = \mathbf{Q}\mathbf{x}^{(t)} = \begin{bmatrix} \theta_1^\top; \dots; \theta_n^\top \end{bmatrix}^\top \in \mathbb{R}^{nd}$: reordered vector of embeddings. $\mathbf{y}^{(t)}$ can also be written as $\mathbf{y}^{(t)} = \begin{bmatrix} \mathbf{y}_c \\ \mathbf{y}_o^{(t)} \end{bmatrix}$.

- $M = Q(I + \alpha P)Q^{-1} \in \mathbb{R}^{nd \times nd}$: reordered update matrix. M can be written by block $M = \begin{bmatrix} M_{cc} & M_{co} \\ M_{oc} & M_{oo} \end{bmatrix}$ where M_{oo} and M_{oc} are submatrices representing outer-to-outer and core-to-outer influences.

D.1 Analysis of SEPAL’s dynamic and analogies to eigenvalue problems

This section presents a theoretical analysis of the SEPAL propagation algorithm. We provide a series of intuitive and structural analogies to classic iterative methods in numerical linear algebra. Our goal is to contextualize the algorithm’s behavior under various assumptions and shed light on its dynamic properties. The analysis is carried out in the case of DistMult, which simplifies the propagation rule due to its element-wise multiplication structure.

SEPAL as power iteration (no normalization, no boundary conditions) We begin by analyzing the case without normalization or fixed embeddings. In this setting, with the vectorized embedding matrix $\mathbf{x}^{(t)} \in \mathbb{R}^{nd}$, the propagation equation (Equation 4) becomes:

$$\mathbf{x}^{(t+1)} = (I + \alpha P)\mathbf{x}^{(t)}, \quad (8)$$

where $P \in \mathbb{R}^{nd \times nd}$ encodes the linear update based on the knowledge graph structure and DistMult composition rule. The matrix P is block diagonal:

$$P = \begin{bmatrix} P^{(1)} & \mathbf{0} & \cdots & \mathbf{0} \\ \mathbf{0} & P^{(2)} & \cdots & \mathbf{0} \\ \vdots & \vdots & \ddots & \vdots \\ \mathbf{0} & \mathbf{0} & \cdots & P^{(d)} \end{bmatrix} \in \mathbb{R}^{nd \times nd}, \quad (9)$$

where each block $P^{(k)}$ corresponds to the k -th embedding dimension and has:

$$P_{u,v}^{(k)} = \sum_{(v,r,u) \in \mathcal{K}} [w_r]_k. \quad (10)$$

$P^{(k)}$ can be seen as a weighted adjacency matrix of the graph, whose weights are the k -th coefficients of the relation embeddings of the corresponding edges. Here, each $(v, r, u) \in \mathcal{K}$ contributes a rank-1 update to P based on w_r .

Therefore, in this setting, the problem is separable with respect to the dimensions, so each dimension can be studied independently.

The recurrence in Equation 8 defines a classical **power iteration**. In general, it diverges unless the spectral radius $\rho(I + \alpha P) < 1$. In our setting, norms can grow arbitrarily because P contains non-normalized adjacency submatrices whose eigenvalues are only bounded by the maximum degree of the graph. In practice, the normalization (studied below) prevents the algorithm from diverging.

With boundary conditions: non-homogeneous recurrence Now, we consider the SEPAL’s setting where core entity embeddings are fixed and only outer embeddings evolve, still without normalization. We use the reordered vector of embeddings $\mathbf{y}^{(t)} = Q\mathbf{x}^{(t)} \in \mathbb{R}^{nd}$, which can be written as follows:

$$\mathbf{y}^{(t)} = \begin{bmatrix} \theta_1^{(t)} \\ \theta_2^{(t)} \\ \vdots \\ \theta_n^{(t)} \end{bmatrix} = \begin{bmatrix} \mathbf{y}_c^{(t)} \\ \mathbf{y}_o^{(t)} \end{bmatrix}, \quad (11)$$

where $\theta_u^{(t)}$ is the embedding of entity u . The reordered update matrix $M = Q(I + \alpha P)Q^{-1}$ has the following block structure:

$$M = \begin{bmatrix} M_{11} & \cdots & M_{1n} \\ \vdots & \ddots & \vdots \\ M_{n1} & \cdots & M_{nn} \end{bmatrix} \in \mathbb{R}^{nd \times nd}, \quad (12)$$

where each block $M_{uv} \in \mathbb{R}^{d \times d}$ encodes how the embedding of entity v contributes to the update of entity u . In the case of the DistMult scoring function, this block is diagonal and takes the form:

$$M_{uv} = \begin{cases} \sum_{(v,r,u) \in \mathcal{K}} \alpha \cdot \text{diag}(\mathbf{w}_r) & \text{if } u \neq v, \\ \mathbf{I}_d + \sum_{(v,r,u) \in \mathcal{K}} \alpha \cdot \text{diag}(\mathbf{w}_r) & \text{otherwise,} \end{cases} \quad (13)$$

where $\text{diag}(\mathbf{w}_r)$ is the diagonal matrix with the relation embedding $\mathbf{w}_r \in \mathbb{R}^d$ on the diagonal.

Thus, M is a sparse block matrix, with each non-zero block being diagonal, and it linearly propagates information across entity embeddings via dimension-wise interactions determined by the DistMult model. Grouping core and outer entities together, we can also write $M = \begin{bmatrix} M_{cc} & M_{co} \\ M_{oc} & M_{oo} \end{bmatrix}$.

This allows us to rewrite the propagation equation to account for the boundary conditions. We obtain:

$$\mathbf{y}_o^{(t+1)} = M_{oo} \mathbf{y}_o^{(t)} + M_{oc} \mathbf{y}_c, \quad (14)$$

where M_{oo} represents signal propagation between outer nodes, and M_{oc} encodes injection from the core nodes.

This is a **non-homogeneous linear recurrence**. If $\rho(M_{oo}) \geq 1$, the outer embeddings diverge in norm. Nonetheless, the structure is analogous to forced linear systems such as:

$$\mathbf{y}_{t+1} = \mathbf{A} \mathbf{y}_t + \mathbf{b},$$

where the long-term behavior is driven by the balance between eigenvalues of \mathbf{A} and direction of \mathbf{b} .

Normalization and Arnoldi-type analogy SEPAL applies ℓ_2 normalization after each update:

$$\boldsymbol{\theta}_u^{(t+1)} = \frac{\boldsymbol{\theta}_u^{(t)} + \alpha \mathbf{a}_u^{(t+1)}}{\|\boldsymbol{\theta}_u^{(t)} + \alpha \mathbf{a}_u^{(t+1)}\|_2}, \quad (15)$$

which constrains every embedding to the unit sphere. This **couple dimensions** and prevents simple linear analysis.

However, the recurrence

$$\mathbf{y}_o^{(t+1)} = M_{oo} \mathbf{y}_o^{(t)} + M_{oc} \mathbf{y}_c, \quad (16)$$

followed by blockwise normalization of $\mathbf{y}^{(t)}$ (with a $\ell_{2,\infty}$ mixed norm), shares structural similarities with the **Arnoldi iteration** (Arnoldi, 1951):

- Successive embeddings span a Krylov subspace: after iteration t , without normalization, $\mathbf{y}_o^{(t)}$ belongs to $\mathcal{K}_t(\mathbf{A}, \mathbf{b}) = \text{span}\{\mathbf{b}, \mathbf{A}\mathbf{b}, \mathbf{A}^2\mathbf{b}, \dots, \mathbf{A}^{t-1}\mathbf{b}\}$, with $\mathbf{A} = M_{oo}$ and $\mathbf{b} = M_{oc}\mathbf{y}_c$, given that $\mathbf{y}_o^{(0)} = \mathbf{0}$.
- Core embeddings define the forcing direction ($\mathbf{b} = M_{oc}\mathbf{y}_c$).
- Normalization serves as a regularizer, preventing divergence in norm.

The Arnoldi iteration is used to compute numerical approximations of the eigenvectors of general matrices, for instance, in ARPACK (Lehoucq et al., 1998). This analogy suggests that the direction of outer embeddings stabilizes over time and aligns with a form of dominant generalized eigenvector of the propagation operator M , conditioned on the core. Therefore, the **embeddings produced by SEPAL's propagation encapsulate global structural information** on the knowledge graph.

D.2 Formal proof of Proposition 4.1

Gradient descent on \mathcal{E} updates the embedding parameters $\boldsymbol{\theta}_u$ of an entity u with

$$\boldsymbol{\theta}_u^{(t+1)} = \boldsymbol{\theta}_u^{(t)} - \eta \frac{\partial \mathcal{E}}{\partial \boldsymbol{\theta}_u^{(t)}} \quad (17)$$

where η is the learning rate.

The mini-batch gradient satisfies

$$\begin{aligned} \frac{\partial \mathcal{E}}{\partial \boldsymbol{\theta}_u^{(t)}} &= - \sum_{(h,r,t) \in \mathcal{B}} \frac{\partial \langle \boldsymbol{\theta}_t^{(t)}, \phi(\boldsymbol{\theta}_h^{(t)}, \mathbf{w}_r) \rangle}{\partial \boldsymbol{\theta}_u^{(t)}} \\ &= - \sum_{\substack{(h,r,t) \in \mathcal{B} \\ h=u}} \frac{\partial \langle \boldsymbol{\theta}_t^{(t)}, \phi(\boldsymbol{\theta}_u^{(t)}, \mathbf{w}_r) \rangle}{\partial \boldsymbol{\theta}_u^{(t)}} - \sum_{\substack{(h,r,t) \in \mathcal{B} \\ t=u}} \frac{\partial \langle \boldsymbol{\theta}_u^{(t)}, \phi(\boldsymbol{\theta}_h^{(t)}, \mathbf{w}_r) \rangle}{\partial \boldsymbol{\theta}_u^{(t)}}, \end{aligned}$$

where \mathcal{B} is the mini-batch. Note that the previous identity is still true if the knowledge graph contains self-loops, due to DistMult’s scoring function being a product. Plugging the DistMult relational operator function $\phi(\boldsymbol{\theta}_h, \mathbf{w}_r) = \boldsymbol{\theta}_h \odot \mathbf{w}_r$ in the previous equation gives

$$\begin{aligned} \frac{\partial \mathcal{E}}{\partial \boldsymbol{\theta}_u^{(t)}} &= - \sum_{\substack{(h,r,t) \in \mathcal{B} \\ h=u}} \frac{\partial \boldsymbol{\theta}_u^{(t)\top} (\mathbf{w}_r \odot \boldsymbol{\theta}_t^{(t)})}{\partial \boldsymbol{\theta}_u^{(t)}} - \sum_{\substack{(h,r,t) \in \mathcal{B} \\ t=u}} \frac{\partial \boldsymbol{\theta}_h^{(t)\top} (\mathbf{w}_r \odot \boldsymbol{\theta}_u^{(t)})}{\partial \boldsymbol{\theta}_u^{(t)}} \\ &= - \sum_{\substack{(h,r,t) \in \mathcal{B} \\ h=u}} \mathbf{w}_r \odot \boldsymbol{\theta}_t^{(t)} - \sum_{\substack{(h,r,t) \in \mathcal{B} \\ t=u}} \boldsymbol{\theta}_h^{(t)} \odot \mathbf{w}_r \\ &= - \sum_{\substack{(h,r,t) \in \mathcal{B} \\ h=u}} \mathbf{w}_r \odot \boldsymbol{\theta}_t^{(t)} - \sum_{\substack{(h,r,t) \in \mathcal{B} \\ t=u}} \phi(\boldsymbol{\theta}_h^{(t)}, \mathbf{w}_r). \end{aligned}$$

Therefore, going back to Equation 17, we get that

$$\boldsymbol{\theta}_u^{(t+1)} = \underbrace{\boldsymbol{\theta}_u^{(t)} + \eta \sum_{\substack{(h,r,t) \in \mathcal{B} \\ t=u}} \phi(\boldsymbol{\theta}_h^{(t)}, \mathbf{w}_r)}_{\text{embedding propagation update for } \eta=\alpha \text{ and } \mathcal{B}=\mathcal{S} \cup \mathcal{C}} + \eta \sum_{\substack{(h,r,t) \in \mathcal{B} \\ h=u}} \mathbf{w}_r \odot \boldsymbol{\theta}_t^{(t)}. \quad (18)$$

We can see that the embedding propagation update only differs by a term that corresponds to the message passing from the tails to the heads. We did not include this term in our message-passing framework because we wanted SEPAL to adapt to any model whose scoring function has the form given by Equation 1. In practice, the propagation direction *tail to head* is already handled by the addition of inverse relations.

Therefore, a parallel can be drawn between: 1) the outer subgraphs and mini batches, 2) the number of propagation steps T and number of epochs, 3) the hyperparameter α and the learning rate.

After each gradient step, we normalize the entity embeddings to enforce the unit norm constraint. This procedure corresponds to **projected gradient descent** on the sphere (Bertsekas, 1997), where each update is followed by a projection (via ℓ^2 normalization) back onto the feasible set. The energy function \mathcal{E} (Equation 5) is composed of inner products and element-wise multiplications of smooth functions, thus it is smooth, and its gradient is Lipschitz continuous on the unit sphere. Under these conditions, the algorithm is guaranteed to converge to a stationary point of the constrained optimization problem (Bertsekas, 1997, Proposition 2.3.2). The limit points of the optimization thus satisfy the first-order optimality conditions on the sphere.

E Presentation and analysis of BLOCS

E.1 Prior work on graph partitioning

Scaling up computation on graph, for graph embedding or more generally, often relies on breaking down graphs in subgraphs. METIS (Karypis and Kumar, 1997), a greedy node-merging algorithm, is a popular solution. A variety of algorithms have also been developed to detect “communities”, groups of nodes more connected together, often with applications on social networks: *Spectral Clustering* (SC) (Shi and Malik, 2000), the *Leading Eigenvector* (LE) method (Newman, 2006), the *Label Propagation Algorithm* (LPA) (Raghavan et al., 2007), the Louvain method (Blondel et al., 2008), the *Infomap* method (Rosvall and Bergstrom, 2008), and the *Leiden* method (Traag et al., 2019) which guarantees connected

communities. LDG (Stanton and Kliot, 2012) and FENNEL (Tsourakakis et al., 2014) are streaming algorithms for very large graphs. Some algorithms have also been specifically tailored for power-law graphs: DBH (Xie et al., 2014) leverages the skewed degree distributions to reduce the communication costs, HDRF (Petroni et al., 2015) is a streaming partitioning method that replicates high-degree nodes first, and Ginger (Chen et al., 2019b) is a hybrid-cut algorithm that uses heuristics for more efficient partitioning on skewed graphs.

E.2 Detailed algorithm and pseudocode

High-level principle We contribute BLOCS, an algorithm designed to break large graphs into Balanced Local Overlapping Conected Subgraphs. The name summarizes the goals: 1) **Balanced**: BLOCS produces subgraphs of comparable sizes. m , the upper bound for subgraph sizes, is a hyperparameter. 2) **Local**: the subgraphs have small diameters. This locality property is important for the efficiency of SEPAL’s propagation phase, as it reduces the number of propagation iterations needed to converge to the global embedding structure. 3) **Overlapping**: a given node can belong to several subgraphs. This serves our purpose because it facilitates information transfer between the different subgraphs during the propagation. 4) **Connected**: all generated subgraphs are connected.

Algorithm 1 BLOCS

Input: Graph $\mathcal{G} = (V, E)$ with nodes V and edges E , hyperparameters h and m
Output: List of overlapping connected subgraphs

$\mathbb{S} \leftarrow \emptyset$ \triangleright list of subgraphs
 $U \leftarrow V$ \triangleright set of unassigned nodes

Step 1: Create subgraphs from super-spreaders’ neighbors
for each node $v \in V$ **do**
 if $\deg(v) > 0.2m$ **then**
 $\mathbb{S}, U \leftarrow \text{SplitNeighbors}(v, \text{max_size} = 0.2m)$
 end if
end for

Step 2: Assign nodes to subgraphs by diffusion
while $|U| > (1-h)|V|$ **do**
 $k \leftarrow 0$; $\mathcal{S}_0 \leftarrow \{\arg \max_{v \in U} \deg(v)\}$ \triangleright start with unassigned node v with highest degree
 while $|\mathcal{S}_k| < 0.8m$ **do**
 $\mathcal{S}_{k+1} \leftarrow \text{Diffuse}(\mathcal{S}_k)$; $k \leftarrow k + 1$
 end while
 Append \mathcal{S}_{k-1} to \mathbb{S} , and update U $\triangleright \mathcal{S}_{k-1}$ is the last subgraph smaller than $0.8m$
end while

Step 3: Merge small overlapping subgraphs
 $\mathbb{S}, U \leftarrow \text{MergeSmallSubgraphs}(\mathbb{S}, \text{min_size} = m/2)$

Step 4: Dilation and diffusion until all entities are assigned
 $p \leftarrow 0$ \triangleright create new subgraphs by diffusion every 5 rounds, to tackle long chains
while $|U| > 0$ **do**
 if 5 divides p and $p > 0$ **then**
 $i \leftarrow 0$
 repeat
 $k \leftarrow 0$; $\mathcal{S}_0 \leftarrow \{\arg \max_{v \in U} \deg(v)\}$
 while $|\mathcal{S}_k| < 0.8m$ **do**
 $\mathcal{S}_{k+1} \leftarrow \text{Diffuse}(\mathcal{S}_k)$; $k \leftarrow k + 1$
 end while
 Append \mathcal{S}_{k-1} to \mathbb{S} , and update U ; $i \leftarrow i + 1$
 until $i = 10$
 end if
 $\mathbb{S} \leftarrow \text{Dilate}(\mathbb{S})$; $p \leftarrow p + 1$
end while

Step 5: Merge small overlapping subgraphs again
 $\mathbb{S}, U \leftarrow \text{SystematicMerge}(\mathbb{S}, \text{min_size} = 0.4m)$

Step 6: Split subgraphs larger than m
 $\mathbb{S}, U \leftarrow \text{SplitLargeSubgraphs}(\mathbb{S}, \text{max_size} = m)$
 $\mathbb{S}, U \leftarrow \text{MergeSmallSubgraphs}(\mathbb{S}, \text{min_size} = m/2)$

Return: \mathbb{S} , the set of overlapping subgraphs covering \mathcal{G}

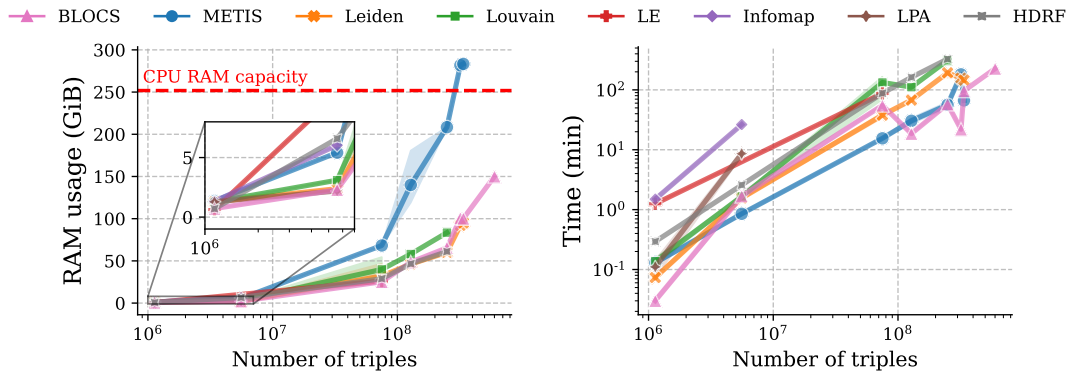


Figure 10: **Scalability of partitioning methods.** Memory usage and time for 8 knowledge graphs of various sizes. The “CPU RAM capacity” dashed line represents the CPU RAM of the machine we used to run SEPAL (we used a different machine with more RAM to run this benchmark, see Appendix B.3). Partitioning methods going beyond this limit thus cannot be combined with SEPAL on our hardware. BLOCS is the only method to scale up to WikiKG90Mv2, a knowledge graph with 601M triples. Leiden and METIS both caused memory errors on WikiKG90Mv2, while HDRF was too long for graphs larger than YAGO4 (our time limit was set to 333 minutes).

BLOCS uses three base mechanisms to grow the subgraphs: **diffuse** (add all neighboring entities to the current subgraph), **merge** (merge two overlapping subgraphs), and **dilate** (add all unassigned neighboring entities to the current subgraph). There are two different regimes during the generation of subgraphs. First, few entities are assigned, and the computationally effective diffusion quickly covers a large part of the graph, especially entities that are close to high-degree nodes. However, once these close entities have been assigned, the effectiveness of diffusion drops because it struggles to reach entities farther away. For this reason, BLOCS switches from diffusion to dilation once the proportion of assigned entities reaches a certain threshold h (a hyperparameter chosen $\approx .6$, depending on the dataset). By adding only unassigned neighbors to subgraphs, dilation drives subgraph growth towards unassigned distant entities. However, the presence of long chains can drastically slow down this regime because they make it add entities one by one. Some knowledge graphs have long chains, for instance YAGO4.5 (see Diameter in Table 2). To tackle them, BLOCS switches back to diffusion for a few steps, with seeds taken inside the long chains.

BLOCS works faster on graphs that have small diameters, where most entities can be reached during the diffusion regime and fewer dilation steps are required (Appendix F.1).

Detailed description Algorithm 1 describes BLOCS pseudocode. Below, we provide more details on subparts of the algorithm.

The function `SplitNeighbors` is designed to manage high-degree nodes by distributing their neighboring entities into smaller subgraphs. For each node whose degree exceeds a certain threshold, it groups its neighbors into multiple subgraphs smaller than this threshold. These new subgraphs also include the original high-degree node to maintain connectedness. By assigning the neighbors of the very high-degree nodes first, BLOCS ensures that subgraphs grow more progressively in the subsequent diffusion step.

The function `MergeSmallSubgraphs` takes a list of subgraphs and a minimum size threshold as input. It identifies subgraphs that are smaller than this given minimum size and merges them into larger subgraphs if they share nodes and if the size of their union remains below the maximum size m .

The function `SystematicMerge` is very similar to `MergeSmallSubgraphs`, but it does not check that the resulting subgraphs are smaller than m . Its objective is to eliminate all the subgraphs whose size is smaller than a given threshold (set to $0.4m$ in Algorithm 1). The subgraphs produced that are larger than m are then handled by the function `SplitLargeSubgraphs`.

The function `SplitLargeSubgraphs` processes the list of subgraphs to break down overly large subgraphs while preserving connectivity. The function iterates over the subgraphs having more than m

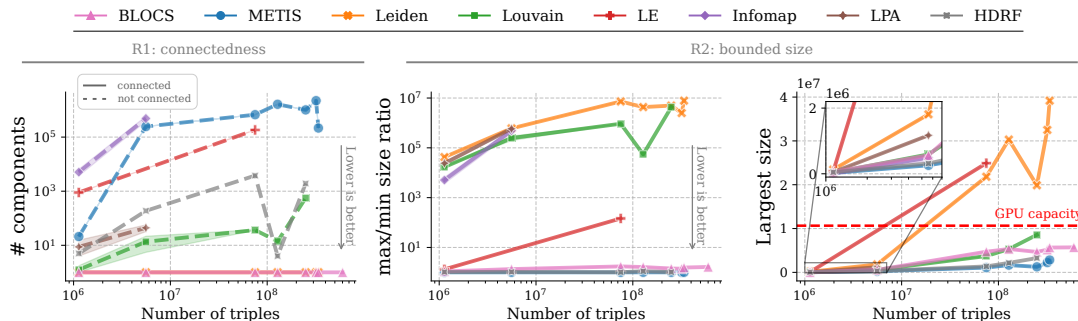


Figure 11: **Quality of partitioning methods.** Maximum number of connected components in one partition, ratio between the largest and smallest partition sizes, and size (number of entities) of the largest partition produced for knowledge graphs of various sizes. The “GPU capacity” dashed line represents the typical number of entities that can be loaded onto the GPU before causing a memory error. Methods producing partitions larger than this cannot be combined with SEPAL, since the partition’s embeddings must fit in GPU memory. BLOCS and Leiden are the only methods to consistently return connected partitions (requirement R1). BLOCS, METIS, and HDRF are the only methods to control the partition size (requirement R2).

nodes, subtracts the core, and computes the connected components. Then, it creates new subgraphs by grouping these connected components until the size limit m is reached. As a result, outer subgraphs can be disconnected at this stage, but merging them with the core ensures their connectedness during embedding propagation.

E.3 Benchmarking BLOCS against partitioning methods

First, we compare BLOCS to other graph partitioning, clustering, and community detection methods. Figure 10 and Figure 11 report empirical evaluation on eight knowledge graphs. BLOCS, METIS, and Leiden are the only approaches that scale to the largest knowledge graphs. Others fail due to excessive runtimes –our limit was set to $2 \cdot 10^4$ seconds. Compared to METIS, BLOCS is more efficient in terms of RAM usage while having similar computation times (Figure 10). Experimental results also show that classic partitioning methods fail to meet the connectedness and size requirements. Indeed, knowledge graphs are prone to yield disconnected partitions due to their scale-free nature: they contain very high-degree nodes. Such a node is hard to allocate to a single subgraph, and subgraphs without it often explode into multiple connected components. Our choice of overlapping subgraphs avoids this problem.

Classic methods do not meet the requirements of SEPAL Here, we provide qualitative observations on the partitions produced by the different methods. We explain why they fail to meet our specific requirements.

METIS is based on a multilevel recursive bisection approach, which coarsens the graph, partitions it, and then refines the partitions. It produces partitions with the same sizes; however, due to the graph structure, they often explode into multiple connected components, which is detrimental to the embedding propagation (see Appendix E.3).

Louvain is based on modularity optimization. It outputs highly imbalanced communities, often with one community containing almost all the nodes and a few very small communities. This imbalance is incompatible with our approach, which requires strict control over the size of the subgraphs so that their embedding fits in GPU memory. Moreover, some of the communities are disconnected. On the two largest graphs, YAGO4 + taxonomy and Freebase, Louvain exceeds the time limit ($2 \cdot 10^4$ seconds).

Leiden modifies Louvain to guarantee connected communities and more stable outputs. It has very good scaling capabilities (Figure 10) but shares with Louvain the issue of producing highly-imbalanced communities.

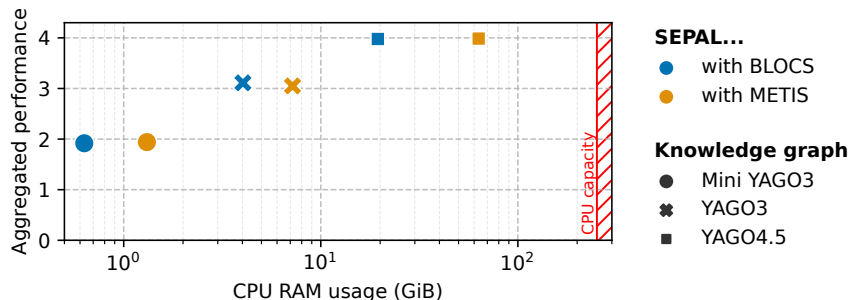


Figure 12: **Ablation study: replacing BLOCS with METIS.** Normalized R2 scores (same as Figure 5) aggregated across evaluation datasets (movie revenues, US accidents, US elections, housing prices) for SEPAL with BLOCS and METIS are plotted against CPU RAM usage. BLOCS necessitates significantly less memory than METIS. We were not able to run SEPAL + METIS on knowledge graphs larger than YAGO4.5, hitting CPU RAM limits during the partitioning stage.

LE is a recursive algorithm that splits nodes based on the sign of their corresponding coefficient in the leading eigenvector of the modularity matrix. If these signs are all the same, the algorithm does not split the network further. Experimentally, LE returns only one partition (containing all the nodes) for YAGO3, YAGO4, YAGO4 + taxonomy, and Freebase. For YAGO4.5 + taxonomy, it hits our pre-set time limit ($2 \cdot 10^4$ seconds). Therefore, we only report its performance for Mini YAGO3 and YAGO4.5, for which it outputs 2 and 4 partitions, respectively. It is important to note that the more communities it returns, the longer it takes to run because the algorithm proceeds recursively.

Infomap uses random walks and information theory to group nodes into communities. Experimentally, it produces a lot of small communities with no connectedness guarantee. Additionally, it is too slow to be used on large graphs.

LPA propagates labels across the network iteratively, allowing densely connected nodes to form communities. Similarly to Louvain and Leiden, the downside is that it does not control the size of the detected communities. It is also too slow to run on the largest graphs.

SC uses the smallest eigenvectors of the graph Laplacian to transform the graph into a low-dimensional space and then applies k-means to group nodes together. However, the expensive eigenvector computation is a bottleneck that does not allow this approach to be used on huge graphs.

HDRF is a streaming algorithm that produces balanced edge partitions (vertex cut) and minimizes the replication factor. However, it produces disconnected partitions, and it is too slow to run on the largest graphs.

Therefore, none of the above methods readily produces subgraphs suitable for SEPAL. Indeed Figure 11 shows that BLOCS is the only method that returns subgraphs that are both connected and bounded in size, while being competitive in terms of scalability (Figure 10).

BLOCS cannot be replaced with METIS To demonstrate the benefits of BLOCS over existing methods, we try to replace BLOCS with METIS in our framework. The results are presented in Figure 12.

Two important points differentiate these methods:

1. Contrary to BLOCS, METIS outputs disconnected partitions (see Figure 11). Given the structure of SEPAL, this results in zero-embeddings for entities not belonging to the core connected component at propagation time. Interestingly, the presence of zero-embeddings affects downstream scores very little, likely because most downstream entities belong to the core connected component and are thus not impacted by this.
2. METIS does not scale as well as BLOCS in terms of CPU memory. On our hardware, SEPAL + METIS could not scale to graphs larger than YAGO4.5 (32M entities), and therefore, BLOCS is indispensable for very large knowledge graphs.

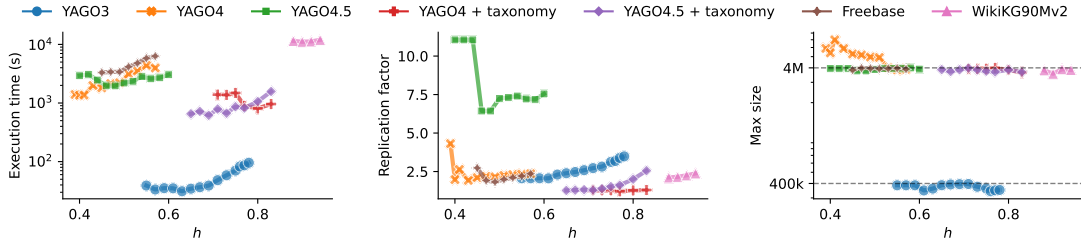


Figure 13: **Sensitivity analysis to parameter h .** Effect of varying h on BLOCS’ execution time, replication factor (average number of outer subgraphs containing a given entity), and maximum subgraph size. A lower bound of the domain of h values to explore for a dataset is given by the proportion of nodes that are neighbors to super-spreaders. Indeed, as BLOCS’ first step is to assign super-spreaders neighbors, if h is smaller than this value, BLOCS completely skips the diffusion phase. For YAGO4.5 and YAGO4, this results in sharp variations of the replication factor or the maximum subgraph size, respectively. The maximum size parameter m was set to 400k for YAGO3, and 4M for others.

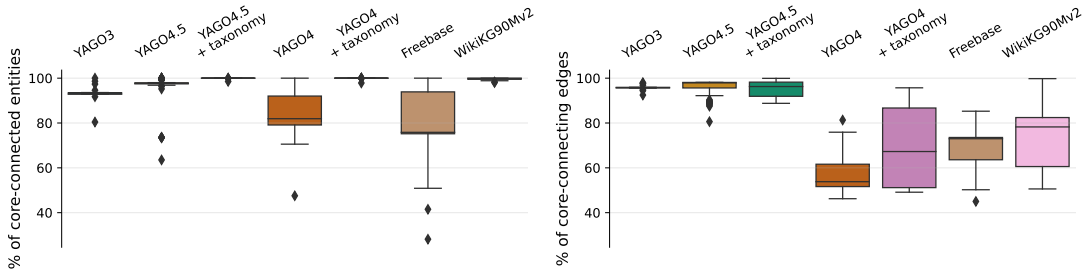


Figure 14: **Outer subgraphs are well connected to the core.** The left plot gives the percentage of outer entities that are directly connected to the core subgraph. The right plot gives the percentage of edges that come from the core subgraph among all the edges coming to a given outer subgraph, showing the amount of information transferred from the core to outer subgraphs relative to outer-outer communication.

E.4 Effect of BLOCS’ stopping diffusion threshold

In the BLOCS algorithm, the hyperparameter h controls the moment of the switch from diffusion to dilation. For $h \in (0, 1)$, BLOCS stops diffusion once the proportion of entities of the graph assigned to a subgraph is greater than or equal to h .

Figure 13 shows that increasing h tends to increase the execution time and the overlap between subgraphs. Higher overlaps can be preferable to enable the information to travel between outer subgraphs during embedding propagation. However, a high overlap also incurs additional communication costs because the embeddings are moved several times from CPU to GPU, increasing SEPAL’s overall execution time.

E.5 How distant from the core are the outer entities?

Figure 14 shows that outer entities are in average very close to the core subgraph. This is due to the fact that the core contains the most central entities, and to the scale-free nature of knowledge graphs.

F Further analysis of SEPAL

F.1 Execution time breakdown

Here, we present the contribution of each part of the pipeline to the total execution time. Specifically, we break down our method into four parts:

1. core subgraph extraction;
2. outer subgraphs generation (BLOCS);
3. core embedding;
4. embedding propagation.

Figure 15 shows the execution time of the different components of SEPAL. It includes six large-scale knowledge graphs, for which the execution times have the same order of magnitude. The results reveal that most of the execution time is due to the core embedding and embedding propagation phases, while the core extraction time is negligible.

Four key factors influence SEPAL’s execution time during the four main steps of the pipeline:

1. **The core selection strategy:** the degree-based selection is faster than the hybrid selection. For the hybrid selection, the factor that influences the speed the most is the number of distinct relations.
2. **The diameter of the knowledge graph:** graphs with large diameters call for more dilation steps during BLOCS’ subgraph generation, and dilation is more costly than diffusion because it requires checking node assignments. This explains why adding the taxonomies to YAGO4 and YAGO4.5 drastically reduces the time required to run BLOCS, as shown on Figure 15.
3. **The core subgraph size:** the more triples in the core subgraph, the longer the core embedding. This explains the wide disparities between the core embedding times on Figure 15, despite all the core subgraphs having roughly the same number of entities: YAGO4 core subgraph is more dense (33M triples), compared to YAGO4.5 (7M triples), for instance. The core embedding time also depends on hyperparameters such as the number of training epochs.
4. **The total number N of entities in the graph:** this number determines the size of the embedding matrix. The communication cost of moving embedding matrices from CPU to GPU, and vice versa, accounts for most of the propagation time, and increases with N . It also increases with the amount of overlap between the outer subgraphs produced by BLOCS, explaining the differences in propagation time between YAGO4.5 and YAGO4.5 + taxonomy for instance.

The number of propagation steps T has little impact on the embedding propagation time. The reason for this is that much of this time stems from the communication cost of loading the embeddings onto the GPU, and not from performing the propagation itself.

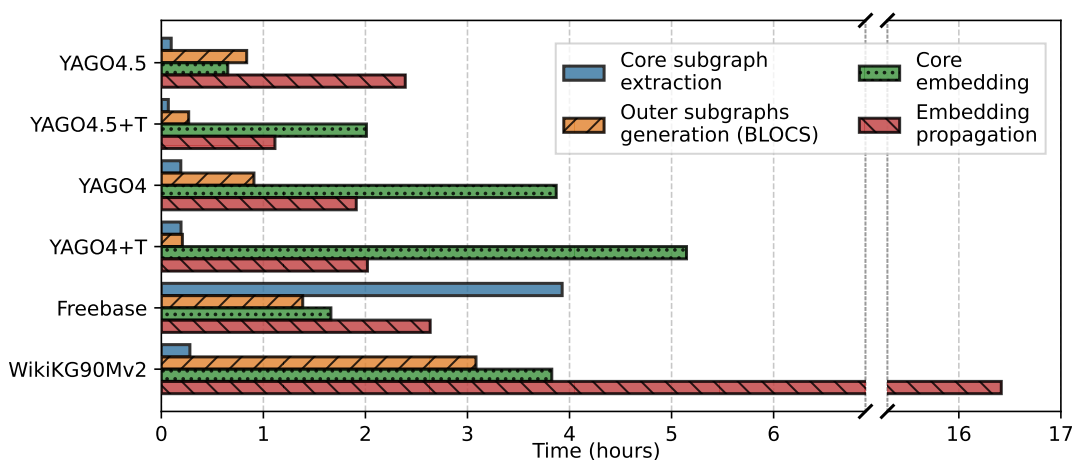


Figure 15: **SEPAL’s execution time breakdown.** Execution time of SEPAL’s different components, for the best-performing configurations of SEPAL on downstream tasks (see Table 7 for hyperparameters values).

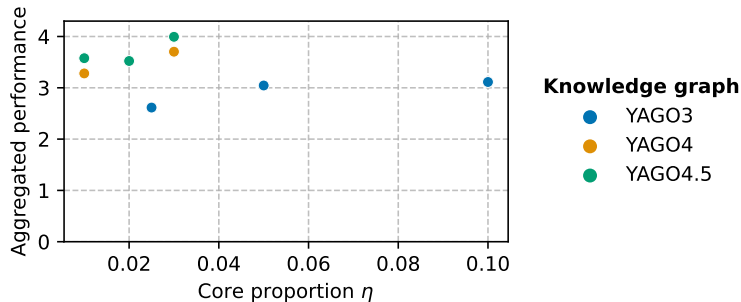


Figure 16: Effect of core proportion η_n on SEPAL’s performance, with the degree-based core selection strategy.

F.2 SEPAL’s hyperparameters

List of SEPAL’s hyperparameters

Here, we list the hyperparameters for SEPAL, and discuss how they can be set. Table 7 gives the values of those that depend on the dataset.

- **Proportion of core nodes η_n** : the idea is to select it large enough to ensure good core embeddings, but not too large so that core embeddings fit in the GPU memory. Figure 16 shows the experimental effect of varying this parameter;
- **Proportion of core edges η_e** : increasing it at the expense of η_n (to keep the core size within GPU memory limits) improves the relational coverage, but reduces the density of the core. Sparser core subgraphs tend to deteriorate the quality of SEPAL’s embeddings for feature enrichment (Figure 20). However a good relational coverage is essential for better link-prediction performance;
- **Stopping diffusion threshold h** : it depends on the graph structure, and tuning is done empirically by monitoring the proportion of unassigned entities during the BLOCS algorithm: h is chosen equal to the proportion of assigned entities at which BLOCS starts to stagnate during its diffusion regime. In practice, Figure 13 and Figure 17 shows that as long as h is chosen greater than the proportion of entities that are neighbors of super-spreaders, the algorithm is not too sensitive to this parameter (otherwise, it skips the diffusion phase, which can be detrimental);
- **Number of propagation steps T** : it is chosen high enough to ensure reaching the remote entities (otherwise, they will have zeros as embeddings). Taking T equal to the graph’s diameter guarantees that this condition is fulfilled. However, for graphs with long chains, this may slow down SEPAL too much. In practice, setting T at 2–3 times the Mean Shortest Path Length (MSPL) usually embeds most entities effectively;
- **Propagation learning rate α** : it controls the proportion of self-information relatively to neighbor-information during propagation updates. For the DistMult model, this parameter has no effect during the first propagation step, when an entity is reached for the first time because outer embeddings are initialized with zeros and the neighbors’ message is normalized. In practice, the embedding of an outer entity can reach in one step a position very close to its fix point, and thus this parameter does not have much effect (Figure 18). For our experiments we typically use $\alpha = 1$;
- **Subgraph maximum size m** : the idea is to use the largest value for which it is possible to fit the subgraph’s embeddings in the GPU memory. We use $4 \cdot 10^4$ for Mini YAGO3, $4 \cdot 10^5$ for YAGO3, $2 \cdot 10^6$ for WikiKG90Mv2, and $4 \cdot 10^6$ for the other knowledge graphs;
- **Embedding dimension d** : we use $d = 100$ (except for complex embeddings, where $d = 50$ to keep the same number of parameters);
- **Number of epochs for core training n_{epoch}** : see Table 7;
- **Batch size for core training b** : see Table 7;
- **Optimizer for core training**: we use the Adam optimizer with learning rate $\text{lr} = 1 \cdot 10^{-3}$;
- **Number p of negative samples per positive for core training**: we use $p = 100$ (Table 7).

Dataset	Parameter	Grid (best in bold)
Mini YAGO3	η_m/η_e	0.05/—, 0.2/—, 0.025/0.005, 0.3/0.05
	h	0.6, 0.65, 0.7, 0.75, 0.8
	T	2, 5 , 10, 15, 25
	n_{epoch}	12, 25, 50, 60, 75
	b	512
	p	1, 100 , 1000
YAGO3	η_m/η_e	0.05/—, 0.1/— , 0.025/0.015, 0.3/0.05
	h	0.55, 0.6, 0.65, 0.7, 0.75, 0.77
	T	2, 5, 10, 15 , 25
	n_{epoch}	16, 18 , 25, 45, 50, 75
	b	2048 , 4096, 8192
	p	1, 100 , 1000
YAGO4.5	η_m/η_e	0.03/—, 0.015/0.01 , 0.05/0.03
	h	0.4, 0.5, 0.6
	T	2, 5, 10, 15, 25, 50
	n_{epoch}	16, 24 , 75
	b	8192 , 16384
	p	1, 100
YAGO4.5+T	η_m/η_e	0.03/— , 0.015/0.005, 0.04/0.015
	h	0.8
	T	2, 5, 10, 15, 20 , 25
	n_{epoch}	32 , 75
	b	8192
	p	100
YAGO4	η_m/η_e	0.03/—, 0.015/0.005 , 0.012/0.025
	h	0.55
	T	2, 5, 10, 15, 20 , 25
	n_{epoch}	4, 28 , 75
	b	8192 , 65536
	p	1, 100
YAGO4+T	η_m/η_e	0.02/—, 0.01/0.005
	h	0.45, 0.8
	T	10, 20
	n_{epoch}	32 , 75
	b	8192 , 65536
	p	1, 100
Freebase	η_m/η_e	0.02/—, 0.01/0.005
	h	0.55
	T	15
	n_{epoch}	24
	b	8192
	p	100
WikiKG90Mv2	η_m/η_e	0.02/—
	h	0.92
	T	10
	n_{epoch}	12
	b	8192
	p	100

Table 7: **Hyperparameter search space** for SEPAL, and best values (in bold) for each knowledge graph on downstream tasks. The best values are those that gave the best average performance on the 4 validation tables and that were used to get the results in Figure 2 and Figure 3.

Experimental study of hyperparameter effect

Figure 16, Figure 17, Figure 18 and Figure 19 investigate the sensitivity of SEPAL to different hyperparameters. The hyperparameter that seems to impact the most SEPAL’s performance is the core proportion η_m . Indeed, Figure 16 shows that increasing η_m tends to improve embedding quality for downstream tasks. However, the effect seems to be plateauing relatively fast for YAGO3 (not much improvement between $\eta_m = 5\%$ and $\eta_m = 10\%$). For other datasets (YAGO4.5, YAGO4), it is not possible to explore larger values of η_m because the core subgraph would not fit in the GPU memory. Moreover,

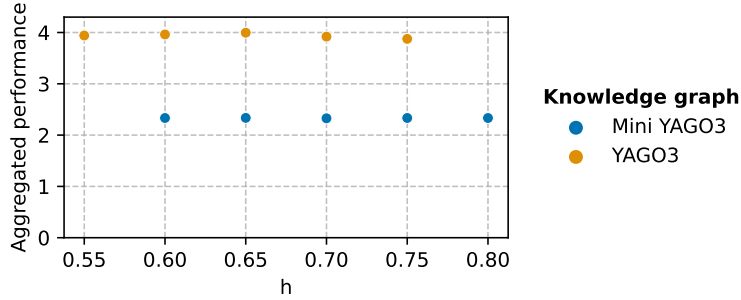


Figure 17: Effect of stopping diffusion threshold h on SEPAL’s performance.

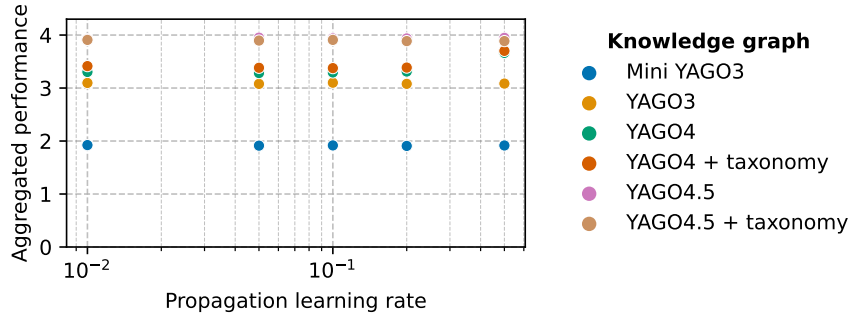


Figure 18: Effect of propagation learning rate α on SEPAL’s downstream performance.

decreasing η_n makes SEPAL run faster, as the core embedding phase accounts for a substantial share of the total execution time (Figure 15). There is, therefore, a trade-off between time and performance.

Core selection strategy *Degree-based selection:* The simple degree-based core selection strategy is convenient for two reasons:

1. Degree is inexpensive to compute, ensuring the core extraction phase to be fast (see Figure 15);
2. It yields very dense core subgraphs. Indeed, while they contain $\eta_n\%$ of the entities of the full graph, they gather around $4\eta_n\%$ of all the triples (Table 8). This allows the training on the core to process a substantial portion of the knowledge-graph triples, resulting in richer representations.

Hybrid selection: However, a problem with the degree-based selection is that some relation types may not be included in the core subgraph. To deal with this issue, SEPAL also proposes a more complex

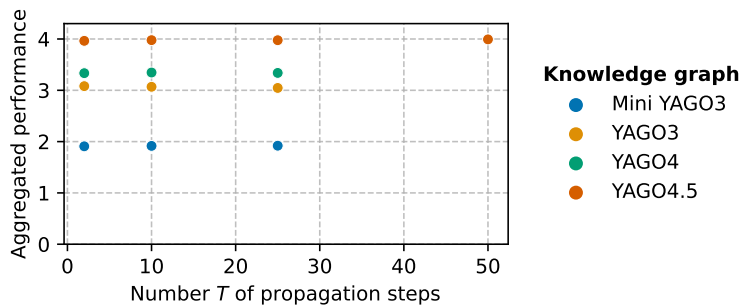


Figure 19: Effect of number T of propagation steps on SEPAL’s downstream performance.

Table 8: **Effect of core selection strategies.** Number of entities and triples inside the core subgraph and proportion of the full graph they represent (in parentheses). η_n and η_e are the hyperparameters for nodes and edges, respectively. Column *#Rel* gives the number of relation types present in the core compared to the total number of relation types in the knowledge graph. We highlight in **red** the cases where some relations are missing. Column *Time* gives the measured computation time for core selection.

	Strategy	η_n	η_e	#Rel	#Entities	#Triples	Time
YAGO3	Degree	5%	-	37/37	126k (4.9%)	1.0M (18.5%)	17s
	Hybrid	2.5%	1.5%	37/37	121k (4.7%)	733k (13.1%)	20s
YAGO4.5	Degree	3%	-	62/62	932k (2.9%)	7.2M (9.6%)	2min
	Hybrid	1.5%	1%	62/62	1.1M (3.3%)	5.7M (7.5%)	6min
YAGO4	Degree	3%	-	61/76	1.1M (3.0%)	33M (13.4%)	8min
	Hybrid	1.5%	0.5%	76/76	1.4M (3.8%)	28M (11.1%)	11min
YAGO4.5+T	Degree	3%	-	64/64	1.5M (3.0%)	13M (9.9%)	4min
	Hybrid	1.5%	0.5%	64/64	1.2M (2.5%)	8.3M (6.5%)	5min
YAGO4+T	Degree	2%	-	64/78	1.3M (2.0%)	41M (12.8%)	9min
	Hybrid	1%	0.5%	78/78	1.5M (2.3%)	32M (10.1%)	12min
Freebase	Degree	2%	-	5,363/14,665	1.7M (2.0%)	15M (4.4%)	9min
	Hybrid	1%	0.5%	14,665/14,665	1.9M (2.3%)	14M (4.1%)	4h
WikiKG90Mv2	Degree	2%	-	886/1,387	1.8M (2.0%)	62M (10.4%)	17min
	Hybrid	0.4%	0.7%	1,387/1,387	2.0M (2.2%)	37M (6.2%)	48min

hybrid method for selecting the core subgraph, that incorporates the relations. It proceeds in four main steps:

1. **Degree selection:** Sample the nodes with the top η_n degrees.
2. **Relation selection:** Sample the edges with the top η_e degrees (sum of degrees of head and tail) for each relation type, and keep the corresponding entities.
3. **Merge:** Take the union of these two sets of entities.
4. **Reconnect:** If the induced subgraph has several connected components, add entities to make it connected. This is done using a breadth-first search (BFS) with early stopping from the node with the highest degree of each given connected component (except the largest) to the largest connected component. For each connected component (except the largest), a path linking it to the largest connected component is added to the core subgraph.

This way, each relation type is guaranteed to belong to the core subgraph, by design. Table 8 confirms this experimentally, even for Freebase and its 14,665 relation types. This method features two hyperparameters η_n and η_e , the proportions for node and edge selections, controlling the size of its output subgraph. The values we used are provided in Table 8 for each dataset.

Regarding performance, Figure 20 shows that the hybrid strategy slightly underperforms the degree-based approach on four real-world downstream tasks. Indeed, the hybrid approach enhances relational coverage but, as a counterpart, yields a sparser core subgraph (see *#Triples* in Table 8), which is detrimental to downstream performance. However, one can adjust the values of η_n and η_e to control the trade-off between downstream performance and relation coverage, depending on the use case. For instance, for the link prediction task, a better relational coverage (greater η_e) improves the performance (Appendix C.4).

F.3 Ablation study: SEPAL without BLOCS

Here, we study the effect of removing BLOCS from our proposed method. On smaller knowledge graphs, SEPAL can be used with a simple core subgraph extraction and embedding followed by the embedding propagation. This ablation reveals the impact of BLOCS on the model’s performance. Figure 21 shows that adding BLOCS to the pipeline on graphs that would not need it (because they are small enough for all the embeddings to fit in GPU memory) does not alter performance. Additionally, BLOCS brings scalability. By tuning the maximum subgraph size m hyperparameter, one can move the

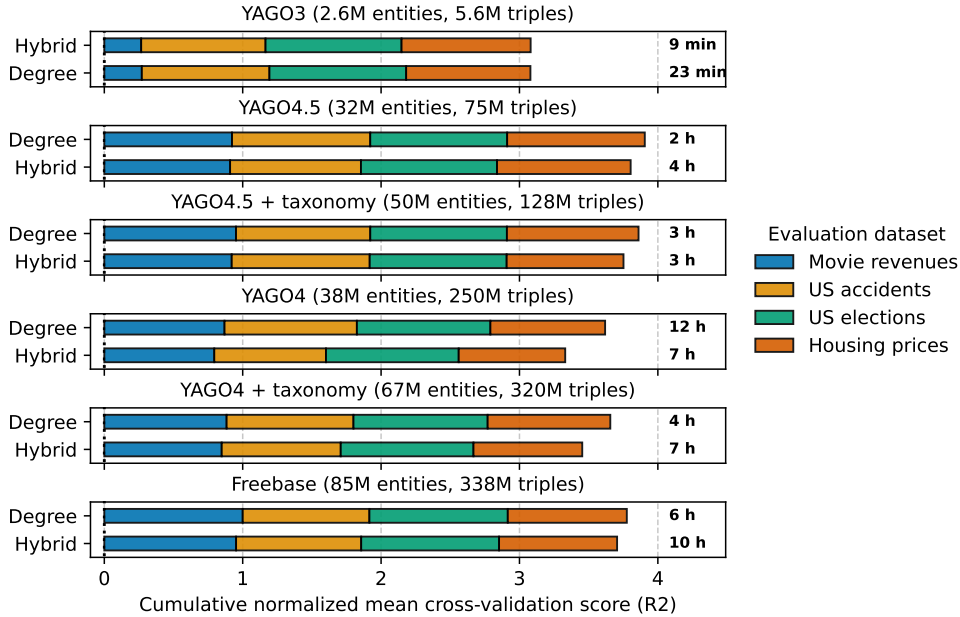


Figure 20: Performance of SEPAL+DistMult for the two different core selection strategies. We use the hyperparameters of Table 8. The simpler degree-based selection strategy runs faster and performs better on downstream tasks.

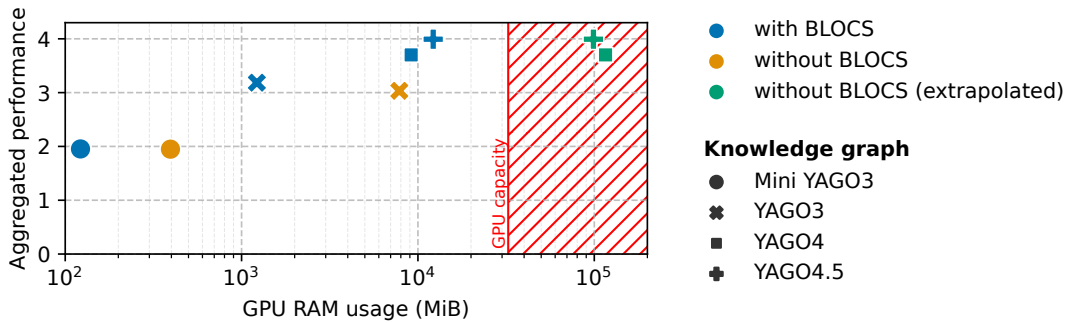


Figure 21: **Ablation study: BLOCS scales SEPAL memory-wise.** Normalized R2 scores aggregated across evaluation datasets (movie revenues, US accidents, US elections, housing prices) for SEPAL with and without BLOCS are plotted against GPU RAM usage. BLOCS preserves performance for a given knowledge graph while drastically reducing memory pressure on GPU RAM. Without BLOCS, the GPU runs out of memory for YAGO4 and YAGO4.5.

blue points horizontally on Figure 21 and choose a value within the GPU memory constraints. There is a trade-off between decreasing GPU RAM usage (*i.e.*, moving the blue points to the left) and increasing execution time, as fewer entities are processed at the same time.

F.4 Speedup over base embedding model

Figure 22 demonstrates that SEPAL can accelerate its base embedding model by more than a factor of 20, while also its boosting performance on downstream tasks.

Moreover, the speedup increases with the number of training epochs, as SEPAL’s constant-cost steps (core extraction, BLOCS, and propagation) are amortized when core training gets longer. Indeed, each additional epoch is cheaper with SEPAL than with DistMult, since training is done only on the smaller core rather than the full graph.

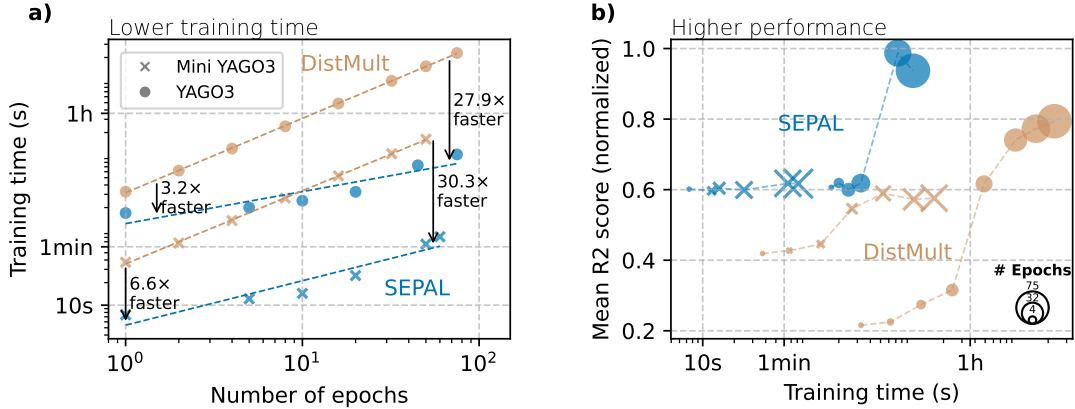


Figure 22: **Comparison between SEPAL and its base embedding model.** **a) Computation time per training iteration.** For a given training configuration, SEPAL is up to 30 times faster than its base embedding algorithm DistMult. **b) Learning curves.** SEPAL achieves strong downstream performance much quicker than DistMult. For both plots, we only vary the number of epochs and fix the following parameters for DistMult’s training and SEPAL’s core training: $p = 1$, $lr = 1 \cdot 10^{-3}$, $b = 512$ for Mini YAGO3 and $b = 2048$ for YAGO3. For SEPAL, we use the degree-based core selection with $\eta_m = 5\%$.

G Discussion

G.1 Comparison between SEPAL and NodePiece

SEPAL shares with NodePiece the fact that it embeds a subset of entities. Parallels can be drawn between: a) the anchors of NodePiece and the core entities of SEPAL; b) the encoder function of NodePiece and the embedding propagation of SEPAL. Yet, our approach differs from NodePiece in several ways.

Neighborhood context handling Both methods handle completely differently the neighborhood of entities. NodePiece tokenizes each node into a sequence of k anchors and m relation types, where k and m are fixed hyperparameters shared by all nodes. If the node degree is greater than m , NodePiece downsamples randomly the relation tokens, and if it is lower than m , [PAD] tokens are appended; both seem sub-optimal. In contrast, SEPAL accommodates any node degree and uses all the neighborhood information, thanks to the message-passing approach that handles the neighborhood context naturally.

Additionally, NodePiece’s tokenization relies on an expensive BFS anchor search, unsuitable for huge graphs. On our hardware, we could not run the vanilla NodePiece (PyKEEN implementation) on graphs bigger than Mini YAGO3 (129k entities). For YAGO3 and YAGO4.5, we had to run an ablated version where nodes are tokenized only from their relational context (i.e., $k = 0$, studied in the NodePiece paper with good results), to skip the anchor search step.

Training procedure At train time, NodePiece goes through the full set of triples at each epoch to optimize both the anchors’ embeddings and the encoder function parameters, necessitating many gra-

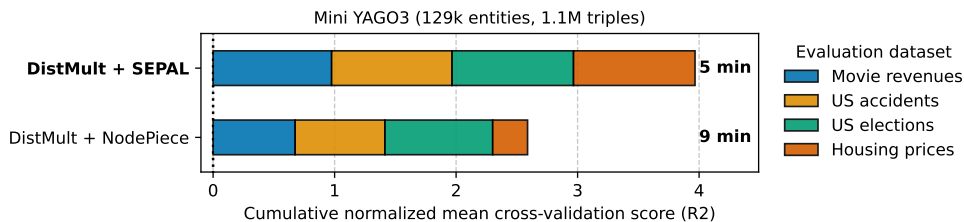


Figure 23: Comparing SEPAL with NodePiece on Mini YAGO3.

dient computes and resulting in long training times for large graphs. On the contrary, SEPAL performs mini-batch gradient descent only on the triples of the core subgraph, which provides significant time savings. To illustrate this, Figure 23 compares the performance of SEPAL and vanilla NodePiece on Mini YAGO3, showing that SEPAL outperforms NodePiece on downstream tasks while being nearly two times quicker.

Embedding propagation to non-anchor/non-core entities To propagate to non-anchor entities, NodePiece uses an encoder function (MLP or Transformer) that has no prior knowledge of the relational structure of the embedding space, and has to learn it through gradient descent. On the contrary, SEPAL leverages the model-specific relational structure to compute the outer embeddings with no further training needed.

G.2 Communication costs of SEPAL

SEPAL optimizes data movement In modern computing architectures, memory transfer costs are high, amounting to much computation, and the key to achieve high operation efficiency is to reduce data movement (Mutlu et al., 2022).

For distributed methods such as PBG or DGL-KE, parallelization incurs additional communication costs due to two factors: 1) Learned parameters shared across workers (relation embeddings) require frequent synchronization 2) Entities occurring in several triples belonging to different buckets have their embeddings moved several times from CPU to GPU, and this for every epoch. This latter effect can be mitigated by better partitioning, but remains significant.

SEPAL avoids much of the communication costs by keeping the core embeddings on GPU memory throughout the process. These core embeddings are the ones that would move the most in distributed settings, because they correspond to high-degree entities involved in many triples. Moreover, SEPAL’s propagation loads each outer subgraph only once on the GPU, contrary to other methods that perform several epochs. This significantly reduces data movement for outer embeddings: empirically, they only cross the CPU/GPU boundary twice on average (see Table 9).

Estimating I/O Communication costs occur in SEPAL during the propagation phase, where the embeddings of each of the subgraphs generated by BLOCS have to be loaded on the GPU, subgraph after subgraph. We analyze the number x of back-and-forth of a given embedding between CPU and GPU memory. The optimal value is $x = 1$, meaning the embeddings are transferred only once. A detailed breakdown follows:

- **For core embeddings:** core embeddings remain at all times on the GPU memory. They are only moved to the CPU once at the end, to be saved on disk with the rest of the embeddings. Therefore, the data movement of core embeddings is optimal: $x_{core} = 1$.
- **For outer embeddings:** SEPAL loads each outer subgraph only once to the GPU. Consequently, the average number x_{outer} of memory transfers for outer embeddings corresponds to the average number of subgraphs in which a given outer entity appears. Table 9 reports empirical values of x_{outer} across datasets, ranging from 1.20 to 7.47, with an overall average of 2.65. This redundancy arises from subgraph overlap, which is directly influenced by the h hyperparameter in BLOCS: smaller values of h yield fewer diffusion steps (and more dilation steps), leading to reduced subgraph overlap and, hence, fewer memory transfers per embedding.

Dataset	x_{outer}
Mini YAGO3	1.20
YAGO3	3.07
YAGO4.5	7.47
YAGO4.5+T	1.94
YAGO4	2.29
YAGO4+T	1.27
Freebase	2.09
WikiKG90Mv2	1.84
Average	2.65

Table 9: Empirical average number of memory transfers between CPU and GPU for outer embeddings across datasets.

The optimal value of $x = 1$ can only be achieved in the case where the entire graph fits in GPU memory. Every approach that scales beyond GPU RAM limits has its communication overheads, i.e., $x > 1$.

For comparison, distributed training schemes that load buckets of triples to GPU iteratively exhibit significantly higher communication costs. In such settings, the number of memory transfers for the embedding of an entity u is given by $x = n_{\text{buckets}}(u) \times n_{\text{epochs}}$ where $n_{\text{buckets}}(u)$ is the number of buckets that contain a triple featuring entity u , and n_{epochs} is the number of epochs. That is at least one or two orders of magnitude greater than what SEPAL achieves in terms of data movement. Indeed, knowledge-graph embedding methods are usually trained for a few tens if not a few hundreds of epochs, so x is much bigger than 10, not even taking into account $n_{\text{buckets}}(u)$ that can be large, depending on the graph structure and on the quality of the graph partitioning.

G.3 Broader impacts

SEPAL may reflect the biases present in the training data. For instance, Wikipedia, from which YAGO is derived, under-represents women (Reagle and Rhue, 2011). We did not evaluate how much our method captures such biases. We note that the abstract nature of embeddings may make the biases less apparent to the user; however, this problem is related to embeddings and not specific to our method. It may be addressed by debiasing techniques (Bolukbasi et al., 2016; Fisher et al., 2020) for which SEPAL could be adapted.